the excitability properties of human motor axons. Brain 2000; 123: 2542–51.

Kiernan MC, Burke D, Andersen KV, Bostock H. Multiple measures of axonal excitability: a new approach in clinical testing. Muscle Nerve 2000; 23: 399–409.

Kiernan MC, Walters RJ, Andersen KV, Taube D, Murray NM, Bostock H, et al. Nerve excitability changes in chronic renal failure indicate membrane depolarization due to hyperkalaemia. Brain 2002a; 125: 1366–78.

Kiernan MC, Guglielmi JM, Kaji R, Murray NM, Bostock H. Evidence for axonal membrane hyperpolarization in multifocal motor neuropathy with conduction block. Brain 2002b; 125: 664–75.

Krajewski KM, Lewis RA, Fuerst DR, Turansky C, Hinderer SR, Garbern J, et al. Neurological dysfunction and axonal degeneration in Charcot–Marie–Tooth disease type 1A. Brain 2000; 123: 1516–27.

Kuwabara S, Ogawara K, Sung J-Y, Mori M, Kanai K, Hattori T, et al. Differences in membrane properties of axonal and demyelinating Guillain–Barré syndromes. Ann Neurol 2002a; 52: 180–7.

Kuwabara S, Kanai K, Sung JY, Ogawara K, Hattori T, Burke D, et al. Axonal hyperpolarization associated with acute hypokalemia: multiple excitability measurements as indicators of the membrane potential of human axons. Muscle Nerve 2002b; 26: 283–7.

Maier M, Berger P, Suter U. Understanding Schwann cell–neurone interactions: the key to Charcot–Marie–Tooth disease? J Anat 2002; 200: 357–66.

Martini R. The effects of myelinating Schwann cells on axons. Muscle Nerve 2001; 24: 456–66.

Peles E, Salzer JL. Molecular domains of myelinated axons. Curr Opin Neurobiol 2000; 10: 558–65.

Priori A, Cinnante C, Pesenti A, Carpo M, Cappellari A, Nobile-Orazio E, et al. Distinctive abnormalities of motor axonal strength–duration

properties in multifocal motor neuropathy and in motor neurone disease. Brain 2002; 125: 2481–90.

Redford EJ, Kapoor R, Smith KJ. Nitric oxide donors reversibly block axonal conduction: demyelinated axons are especially susceptible. Brain 1997; 120: 2149–57.

Robaglia-Schlupp A, Pizant J, Norreel JC, Passage E, Saberan-Djoneidi D, Ansaldi JL, et al. PMP22 overexpression causes dysmyelination in mice. Brain 2002; 125: 2213–21.

Sahenk Z, Mendell JR. Alterations in nodes of Ranvier and Schmidt–Lanterman incisures in Charcot–Marie–Tooth neuropathies. Ann NY Acad Sci 1999a; 883: 508–12.

Sahenk Z, Chen L, Mendell JR. Effects of PMP22 duplication and deletions on the axonal cytoskeleton. Ann Neurol 1999b; 45: 16–24.

Scherer SS, Arroyo EJ. Recent progress on the molecular organization of myelinated axons. J Peripher Nerv Syst 2002; 7: 1–12.

Sung J-Y, Kuwabara S, Kaji R, Ogawara K, Mori M, Kanai K, Nodera H, Hattori T, Bostock H. Altered nerve membrane properties at the wrist correlate with clinical profiles in chronic inflammatory demyelinating polyneuropathy. Muscle Nerve 2004; in press.

Vabnick I, Trimmer JS, Schwarz TL, Levinson SR, Risal D, Shrager P. Dynamic potassium channel distributions during axonal development prevent aberrant firing patterns. J Neurosci 1999; 19: 747–58.

Yang Q, Kaji R, Hirota N, Kojima Y, Takagi T, Kohara N, et al. Effect of maturation on nerve excitability in an experimental model of threshold electrotonus. Muscle Nerve 2000; 23: 498–506.

Yang Q, Kaji R, Takagi T, Kohara N, Murase N, Yamada Y, et al. Abnormal axonal inward rectifier in streptozocin-induced experimental diabetic neuropathy. Brain 2001; 124: 1149–55.

Leuprorelin rescues polyglutamine-dependent phenotypes in a transgenic mouse model of spinal and bulbar muscular atrophy

Masahisa Katsuno, Hiroaki Adachi, Manabu Doyu,
Makoto Minamiyama, Chen Sang, Yasushi Kobayashi, Akira Inukai
& Gen Sobue

nature
medicine

Leuprorelin rescues polyglutamine-dependent phenotypes in a transgenic mouse model of spinal and bulbar muscular atrophy

Masahisa Katsuno, Hiroaki Adachi, Manabu Doyu, Makoto Minamiyama, Chen Sang, Yasushi Kobayashi, Akira Inukai & Gen Sobue

Spinal and bulbar muscular atrophy (SBMA) is an adult-onset motor neuron disease that affects males. It is caused by the expansion of a polyglutamine (polyQ) tract in androgen receptors. Female carriers are usually asymptomatic. No specific treatment has been established. Our transgenic mouse model carrying a full-length human androgen receptor with expanded polyQ has considerable gender-related motor impairment. This phenotype was abrogated by castration, which prevented nuclear translocation of mutant androgen receptors. We examined the effect of androgen-blockade drugs on our mouse model. Leuprorelin, a lutenizing hormone–releasing hormone (LHRH) agonist that reduces testosterone release from the testis, rescued motor dysfunction and nuclear accumulation of mutant androgen receptors in male transgenic mice. Moreover, leuprorelin treatment reversed the behavioral and histopathological phenotypes that were once caused by transient increases in serum testosterone. Flutamide, an androgen antagonist promoting nuclear translocation of androgen receptors, yielded no therapeutic effect. Leuprorelin thus seems to be a promising candidate for the treatment of SBMA.

SBMA, also known as Kennedy disease, is an adult-onset motor neuron disease characterized by proximal muscle atrophy, weakness, contraction fasciculations and bulbar involvement[1,2]. This disorder affects males; female carriers are usually asymptomatic[3,4,5]. No specific treatment for SBMA has been established.

The molecular basis of SBMA is the expansion of a trinucleotide CAG repeat encoding the polyQ tract in the first exon of the androgen receptor gene[6]. The CAG repeat within androgen receptor genes ranges in size from 5 to 33 repeats in normal subjects, but from 40 to 62 in patients with SBMA[7]. There is an inverse correlation between the CAG repeat size and the age at onset, or the disease severity adjusted by the age at examination in SBMA[8,9] as well as other polyQ diseases[10].

The cardinal pathological finding in SBMA is nuclear inclusions containing mutant and truncated androgen receptors with expanded polyQ tracts in the residual motor neurons of the brain stem and spinal cord[11] and some other visceral organs[12]. The presence of nuclear inclusions is also a pathological hallmark in most other polyQ diseases, and is considered to be relevant to pathophysiology[10]. Although the entire mechanism of polyQ-induced neuronal dysfunction and subsequent cell loss has not been clarified, nuclear localization of the mutant protein could be essential in the pathogenesis of polyQ diseases[13,14].

A transgenic mouse model was designed that expresses the full-length human androgen receptor containing 24 or 97 CAG repeats under the control of a cytomegalovirus enhancer and a chicken β-actin promoter[15]. Although no transgenic lines with 24 CAG repeats manifested any characteristic SBMA phenotypic traits, three of five lines

with 97 CAG repeats (AR-97Q) showed progressive motor impairment, which was notably pronounced and accelerated in male AR-97Q mice, but was not noted or was far less severe in female AR-97Q mice. Thus, this model recapitulated not only the neurologic disorder, but also the phenotypic difference with gender that is a feature specific to SBMA. Nuclear localization of mutant androgen receptors was considerable in the male transgenic mice but not in the females, in agreement with the gender-related phenotypic expression. Castrated male AR-97Q mice showed considerable improvement in symptoms, pathological findings and nuclear localization of the mutant androgen receptors, whereas testosterone caused notable exacerbation in female AR-97Q mice, indicating that large amounts of serum testosterone were essential for the phenotypic expression of SBMA, and that testosterone deprivation conferred therapeutic effects in this disease.

Here we examined the effect of two androgen-blockade drugs used in the treatment of prostate cancer. Although flutamide had no effect on the phenotypic expression of SBMA, leuprorelin reversed both the symptomatic and histopathological phenotypes. Our results indicate that ligand-dependent nuclear translocation of mutant androgen receptors is the main source of the pathogenesis of SBMA, and that leuprorelin suppresses this translocation.

RESULTS

Leuprorelin rescues the phenotypic expression of SBMA

Leuprorelin-treated male AR-97Q mice showed considerable amelioration of symptoms, pathological findings and nuclear localization of
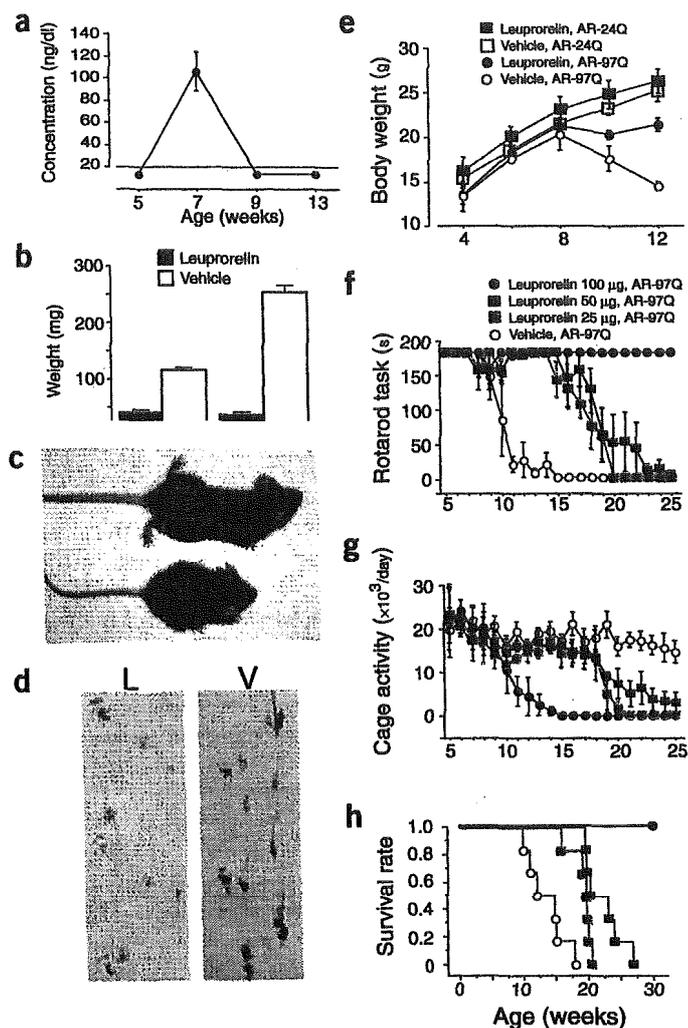
Figure 1 Effects of leuprorelin on symptoms in male AR-97Q mice.
(a) Serum testosterone in AR-97Q mice ($n = 6$). (b) Weights of prostates and seminal vesicles of 13-week-old #4-6 mice. (c) The leuprorelin-treated AR-97Q male mouse (top) did not show the muscular atrophy seen in the vehicle-treated male mouse (bottom; 12-week-old #4-6 mice).
(d) Footprints of 12-week-old leuprorelin-treated (L) and vehicle-treated (V) male AR-97Q #4-6 mice . Red, front paw; blue, hind paws. (e) Effect of leuprorelin on body weight in AR-24Q #5-5 and AR-97Q #7-8 mice.
(f–h) Rotarod task (f), cage activity (g) and survival rates (h) of AR-97Q #7-8 mice. Key applies to f–h.

the transgene protein compared with vehicle-treated AR-97Q mice. Leuprorelin initially increased serum testosterone by exerting agonist effects at the LHRH receptor, but subsequently reduced it to undetectable amounts (Fig. 1a). The androgen blockade was also confirmed by the decreased weights of the prostate and seminal vesicles ($P < 0.001$ for both; Fig. 1b). This reduction was indistinguishable from that in castrated mice (data not shown). Leuprorelin caused infertility in both male AR-97Q mice and normal littermates at a dose of 100 μg, although the mice were fertile at doses of 25 or 50 μg leuprorelin. The leuprorelin-treated AR-97Q mice showed notable amelioration of muscle atrophy and reduced body size (Fig. 1c). By footprint analysis, the vehicle-treated AR-97Q mice had motor weakness and dragged their hind legs, but these symptoms were substantially attenuated by leuprorelin treatment (Fig. 1d). Leuprorelin treatment profoundly suppressed progressive emaciation, which was evident in the vehicle-

treated mice (Fig. 1e). Although it is known to increase body mass in human subjects, leuprorelin did not induce significant obesity in male AR-24Q mice (Fig. 1e). The leuprorelin-treated male mice had significantly ($P < 0.0001$) less or almost no motor impairment, as assessed by rotarod task and cage activity (Fig. 1f,g). Leuprorelin also significantly ($P=0.0005$) prolonged life (Fig. 1h). Although the effect on fertility could be abrogated by dose reduction, the therapeutic effects of leuprorelin were insufficient at a lower dose (Fig. 1f–h).

By western blot analysis of total tissue homogenate or nuclear fraction, leuprorelin-treated male AR-97Q mice had many fewer mutant androgen receptors smearing from the top of the gel than did vehicle-treated male mice (Fig. 2a,b). This indicated that leuprorelin successfully reduced insoluble nuclear androgen receptor fragments. The leuprorelin-treated mice had much less diffuse nuclear staining and fewer nuclear inclusions detected with the 1C2 antibody to polyQ (Fig. 2c). Muscle histology showed considerable amelioration of neurogenic muscle atrophy, such as grouped atrophy and small angulated fibers, with leuprorelin treatment (Fig. 2c).

Testosterone given to mice from 13 weeks of age substantially aggravated the neurological symptoms (Fig. 3a,b) and pathological findings by immunohistochemistry with 1C2 (Fig. 3c) of leuprorelin-treated AR-97Q mice.

Leuprorelin reverses symptomatic and pathological phenotypes

Leuprorelin-treated AR-97Q mice showed a decrease in body weight and deterioration in the rotarod task at an age of 8–9 weeks (Figs. 1e,f and 3a), when serum testosterone initially increased through the agonistic effect of leuprorelin (Fig. 1a). This change was transient and was followed by sustained amelioration along with consequent suppression of testosterone production. Footprint analysis also showed temporary exacerbation of motor impairment (Fig. 4a). Immunostaining of tail specimens obtained from the same mouse showed an increase in the number of the muscle fibers at 4 weeks of leuprorelin administration by nuclear 1C2 staining, although this staining was diminished by another 4 weeks of treatment. Vehicle-treated AR-97Q mice showed robust deterioration of nuclear 1C2 staining (Fig. 4b,c).

Flutamide does not suppress SBMA phenotype

In contrast, flutamide treatment did not ameliorate the symptoms, pathological features or nuclear localization of the mutant androgen receptors in male transgenic mice. Flutamide significantly ($P < 0.0001$) decreased the weights of the prostate and seminal vesicles (Fig. 5a). There was no significant difference in the androgen-blockade effects of leuprorelin and flutamide. Flutamide treatment of male AR-97Q mice did not ameliorate muscle atrophy or body size reduction (Fig. 5b). By footprint analysis, both flutamide-treated and vehicle-treated mice showed motor weakness and dragged their hind legs (Fig. 5c). Both flutamide-treated and vehicle-treated male AR-97Q mice showed progressive emaciation (Fig. 5d). Flutamide had no effect on the rotarod task, cage activity or life span (Fig. 5e–g).

Western blot analysis showed mutant androgen receptors smearing from the top of the gel in whole-tissue homogenates of both flutamide-treated and vehicle-treated mice (Fig. 6a). These mutant androgen receptors localized in the nuclear fraction (Fig. 6b). Flutamide-treated mice showed no diminution in diffuse nuclear staining or nuclear inclusions (Fig. 6c).

DISCUSSION

Our study shows that leuprorelin rescues symptomatic and pathological phenotypes in our transgenic mouse model of SBMA. Leuprorelin prevents testicular testosterone production by downregulating LHRH
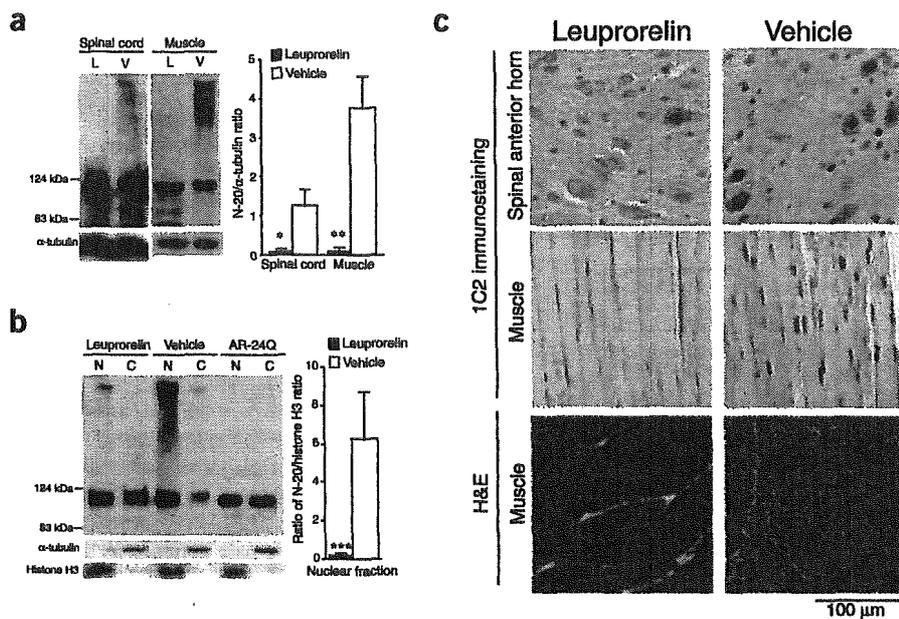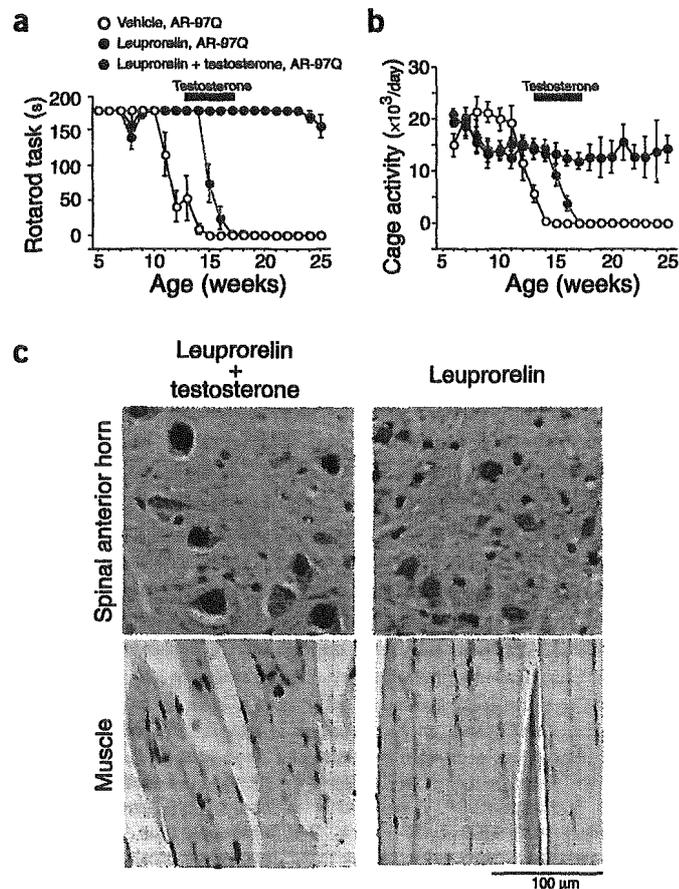
Figure 2 Effects of leuprorelin on mutant androgen receptor expression and neuropathology in male AR-97Q mice. (a) Western blot analysis with an antibody to androgen receptor (N-20) of total homogenates of the spinal cords and muscles of 13-week-old leuprorelin-treated (L) and vehicle-treated (V) male AR-97Q #7-8 mice. *, $P = 0.011$; **, $P = 0.015$. Left margin, molecular sizes. Bottom, α-tubulin (control blot). (b) Western blot analysis with N-20 of nuclear (N) and cytoplasmic (C) fractions of muscles of the male mice (13 weeks old; #7-8) given leuprorelin (L) or vehicle (V) and a transgenic mouse (13 weeks old; #5-5) with androgen receptors with 24 CAG repeats (AR-24Q). Smearing of mutant androgen receptors was present in the nuclear fraction lanes. ***, $P < 0.0001$. Left margin, molecular sizes. Bottom, accuracy of fractionation confirmed with a nuclear marker (histone H3) and a cytoplasmic marker (α-tubulin). (c) Immunohistochemical study with 1C2, showing diffuse nuclear staining and nuclear inclusions in the spinal anterior horns and muscles of 13-week-old male leuprorelin-treated and vehicle-treated AR-97Q #7-8 mice and H&E staining of the muscle of vehicle-treated and leuprorelin-treated male mice.
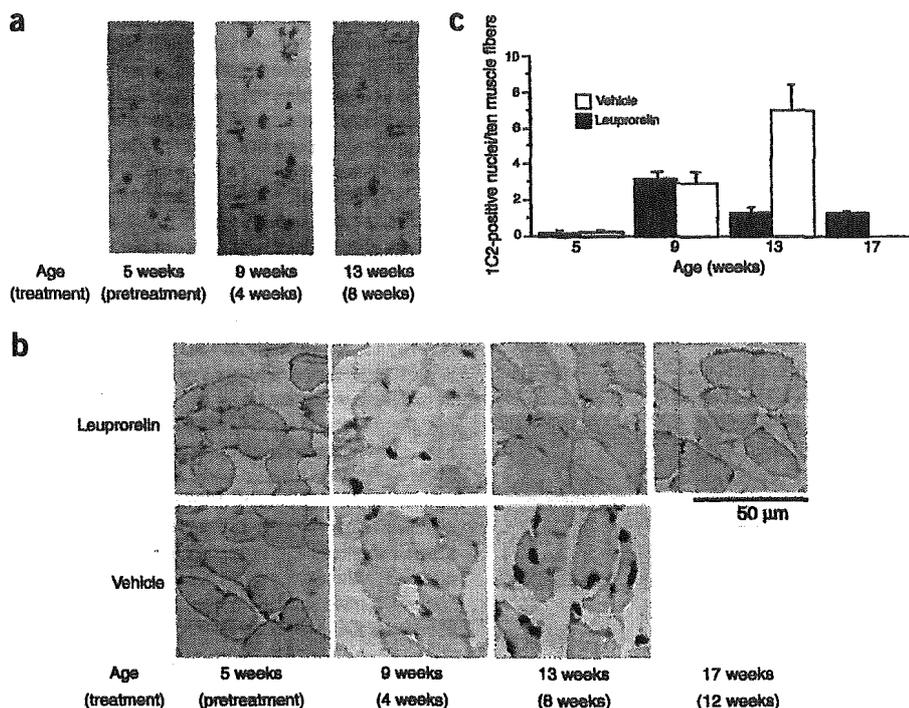
receptors in the pituitary, and has been used extensively for medical castration in the therapy of prostate cancer, based on the androgen sensitivity of the tumor[16]. Its safety and tolerability have been widely approved, although it has possible side effects, including decreased libido, impotence, hot flushes, osteoporosis and fatigue. Here, fertility was decreased in leoprorelin-treated mice, and this effect was nullified by dose reduction. Leuprorelin decreases plasma testosterone by 95% or more[17]. Blockade of testosterone production was apparent in our transgenic mouse model and, furthermore, testosterone exacerbated phenotypic expression in leuprorelin-treated male transgenic mice. These findings indicated that suppression of testosterone was responsible for the therapeutic effect of leuprorelin. Ligand-dependent nuclear translocation of androgen receptor may be involved in the pathogenesis of SBMA[15]; here, leuprorelin seemed to prevent mutant androgen receptor translocation and suppressed its nuclear accumulation and subsequent neuronal dysfunction. Indeed, both western blot analysis and immunostaining with 1C2 antibody showed that leuprorelin substantially reduced nuclear accumulation of mutant androgen receptors. Leuprorelin could be a promising therapeutic agent for SBMA, given its minimal invasiveness and established safety. In clinical trials, however, the patient's desire for fertility should be taken into account, and the appropriate clinical dose should be carefully determined with reference to our dose-response study.

As leuprorelin initially acts as an LHRH agonist, serum testosterone temporarily increased after 2 weeks of treatment in our transgenic mice. As expected from this initial testosterone surge, nuclear staining with antibody to polyQ and motor dysfunction of the mice deteriorated in the early stage of leuprorelin therapy. Nevertheless, serial observations of tail specimens showed that nuclear accumulation of mutant androgen receptors was transient and was actually reversed by sustained leuprorelin treatment. Behavioral tests also demonstrated

immediate recovery of motor function after initial deterioration, and long-term stabilization of neurologic function was achieved by leuprorelin treatment. The reversibility of polyQ pathogenesis has also been shown by turning off gene expression in an inducible mouse model of Huntington disease[18]. Our results, however, indicated that preventing nuclear translocation of mutant androgen receptors was

Figure 3 Effects of testosterone in leuprorelin-treated male AR-97Q mice. (a,b) Rotarod task (a) and cage activity (b) of male AR-97Q #4-6 mice treated with leuprorelin ($n = 6$) or leuprorelin plus testosterone ($n = 6$; time of testosterone administration indicated by bar in graph). (c) Immunostaining with 1C2, showing diffuse nuclear staining and nuclear inclusions in the spinal anterior horns and muscles of 17-week-old leuprorelin-treated and testosterone-treated AR-97Q male #4-6 mice.

function[26]. Thus, the neurologic impairment in SBMA cannot be attributed to the loss of androgen receptor function[27]. SBMA has been considered an X-linked disease, whereas other polyQ diseases show autosomal dominant inheritance. If the toxic gain of mutant androgen receptor function is the main pathogenic process in SBMA, symptoms should be manifested in female patients, as in other polyQ diseases. Female patients, however, rarely have clinically characteristic phenotypes, even if they are homozygous[3–5]. Thus, SBMA symptoms are manifested only in the presence of large amounts of serum testosterone, as in male patients. This hypothesis is supported by the finding that female transgenic mice showed subtle phenotypic expression that was amplified by testosterone administration[15]. Taken together, the ligand effect,

enough to reverse both symptomatic and pathological phenotypes in our transgenic mice. As the pathophysiology of AR-97Q mice is neuronal dysfunction without neuronal cell loss[15], our results indicated that polyQ pathogenesis was reversible at least in its dysfunctional stage. We need to determine the early dysfunctional period in human polyQ diseases.

In contrast to the notable success of leuprorelin therapy, flutamide produced no beneficial effects despite its sufficient antiandrogen effects. Flutamide, the first androgen antagonist discovered, has very specific affinity for androgen receptors, and competes with testosterone for binding to the receptor. It has been used to treat prostate cancer, usually in association with an LHRH agonist, to block the action of adrenal testosterone[17,19]. Although flutamide suppresses the androgen-dependent transactivation, it does not reduce plasma testosterone. Furthermore, flutamide does not inhibit, but may even facilitate, the nuclear translocation of androgen receptors[20,21]. Flutamide also promoted nuclear translocation of mutant androgen receptors containing expanded polyQ in cell and Drosophila models of SBMA[22,23]. This may be the reason flutamide produced no therapeutic effect in our transgenic mouse model of SBMA. Flutamide is not likely to be a therapeutic agent for SBMA.

As in other polyQ diseases, a toxic gain of mutant androgen receptor function has been considered the main cause of the pathogenesis of SBMA[24]. Although the expansion of polyQ tract inhibits the transcriptional activities of androgen receptors and promotes androgen receptor degradation[25], motor impairment has not been noted in patients with severe testicular feminization lacking androgen receptor
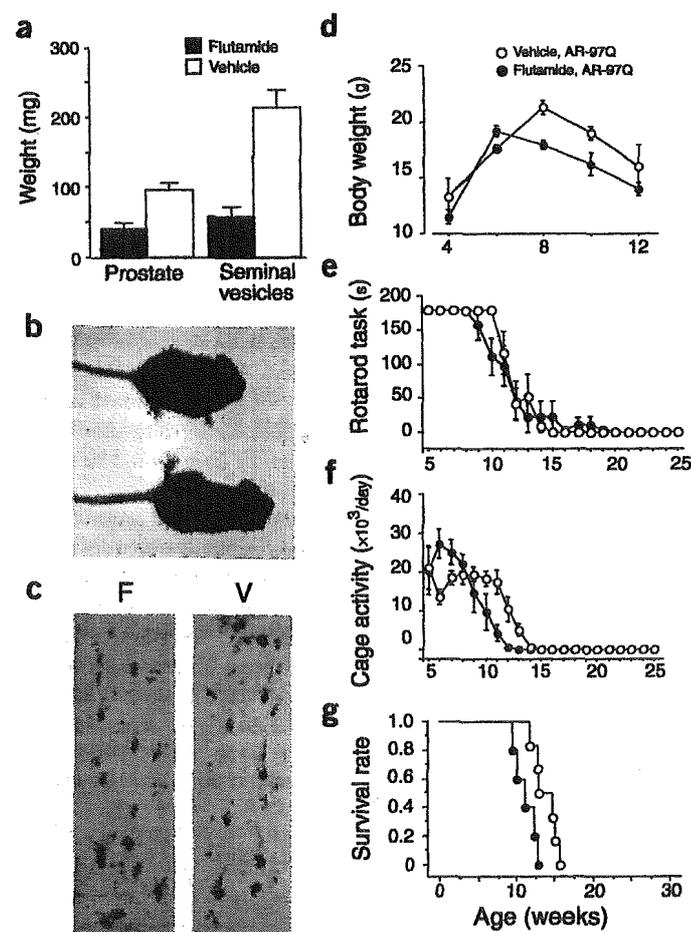
Figure 5 Effects of flutamide on the symptoms of male AR-97Q mice.
(a) Weights of prostates and seminal vesicles of 12-week-old #4-6 mice.
(b) Flutamide-treated (top) and vehicle-treated male mice (11-week-old #4-6 mice). (c) Footprints of 11-week-old flutamide-treated (F) and vehicle-treated (bottom) male AR-97Q #4-6 mice . Red, front paws; blue, hind paws. (d-g) Body weights, rotarod tasks, cage activity and survival rates of flutamide-treated (n = 6) and vehicle-treated (n = 6) male AR-97Q #4-6 mice.
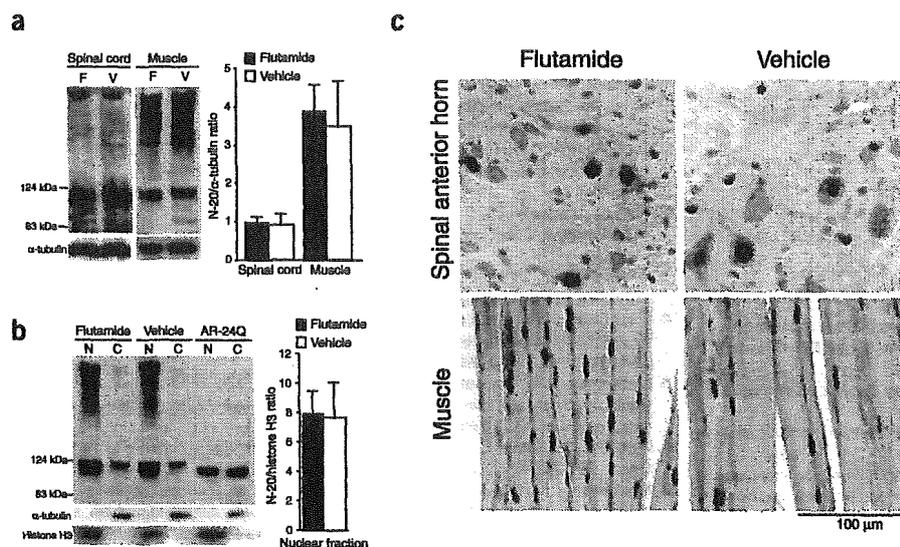
Figure 6 Effects of flutamide on mutant androgen receptor expression and neuropathology in male AR-97Q mice. (a) Western blot analysis with an antibody to androgen receptor (N-20) of total homogenates from the spinal cords and muscles of 13-week-old flutamide-treated (F) and vehicle-treated (V) male AR-97Q #7-8 mice . Left margin, molecular sizes. Bottom, α-tubulin (control blot). (b) Western blot analysis with N-20 of nuclear (N) and cytoplasmic (C) fractions from the muscles of 13-week-old #7-8 male mice given flutamide (F) or vehicle (V), and a 13-week-old transgenic mouse with androgen receptors with 24 CAG repeats (AR-24Q; #5-5). Left margin, molecular sizes. Bottom, accuracy of fractionation confirmed with a nuclear marker (histone H3) and a cytoplasmic marker (α-tubulin). (c) Immunostaining with 1C2, showing diffuse nuclear staining and nuclear inclusions in the spinal anterior horns and muscles of flutamide-treated and vehicle-treated mice (12-week-old #4-6 mice).

rather than protein expression of mutant androgen receptors is important in SBMA pathogenesis and provides a theoretical basis for the treatment effects.

Although there have been no notably effective therapeutic approaches to polyQ diseases, some promising results have been reported using transgenic animal models. Molecular chaperones, which renature misfolded mutant proteins, have exerted beneficial effects in cell and animal models of polyQ diseases. Heat-shock protein (HSP) 70 and HSP40 yielded preventive effects in a SBMA cell model[28]. Overexpression of HSP70 had preventive effects in our transgenic mouse model of SMBA[29] as well as in SCA1 cell and transgenic mouse models[30,31]. Increasing the expression of or enhancing the function of molecular chaperones could also be a potential therapy for SBMA. Alternatively, histone deacetylase inhibitor suppresses polyQ toxicity in cell and *Drosophila* models[32,33], but its effect is not sufficient in a mouse model of Huntington disease[34]. An ideal treatment for polyQ diseases could be a combination of these and other therapeutic strategies. Our study has indicated that hormonal therapy with LHRH agonist, such as leuprorelin, could be central to SBMA therapy.

METHODS

Generation and maintenance of transgenic mice. We generated AR-24Q and AR-97Q mice as described before[15]. We subcloned a full-length human androgen receptor fragment containing 24 or 97 CAG repeats[35] into a pCAGGS vector[36] digested with *Hin*dIII, microinjected the result into fertilized eggs of BDF1 mice and obtained five founders with AR-97Q. We maintained these mouse lines by back-crossing with C57Bl/6J. We examined all the symptomatic lines (#2-6, #4-6, #7-8). All animal experiments were approved by the Animal Care Committee of Nagoya University Graduate School of Medicine.

Neurological and behavioral testing. We analyzed the rotarod task in mice using an Economex Rotarod (Colombus Instruments) and measured cage activity with the AB system (Neuroscience, Tokyo, Japan) as described before[15,37].

Hormonal intervention and serum testosterone assay. We injected leuprorelin acetate (provided by Takeda Pharmaceutical) subcutaneously at a dose of 25, 50 or 100 μg per mouse every 2 weeks from 5 weeks of age. We administered leuprorelin at a dose of 100 μg unless otherwise indicated. We injected control AR-97Q male mice with a vehicle containing D-mannitol, carmellose sodium and polysolvate 80. We gave leuprorelin-treated AR-97Q mice either leuprorelin only or leuprorelin plus 20 μg testosterone enanthate dissolved in sesame oil (injected subcutaneously) weekly from the age of 13 weeks. We dis-

solved flutamide (Sigma-Aldrich) in 10% ethanol and 90% sesame oil, and gave it at a dose of 1.8 mg per mouse once every second day[38]. We injected the control AR-97Q male mice with vehicle. We assayed serum testosterone with the Coat-A-Count Total Testosterone radioimmunoassay (Diagnostic Products Corporation).

Protein expression analysis. We exsanguinated mice anesthetized by ketamine-xylazine, and 'snap-froze' their tissues with powdered CO_2 in acetone. We homogenized the tissues (2,500g for 15 min at 4 °C) in 50 mM Tris, pH 8.0, 150 mM NaCl, 1% Nonidet-P40, 0.5% deoxycholate, 0.1% SDS and 1 mM 2-mercaptoethanol with 1 mM PMSF and 6 μg/ml aprotinine. We loaded each lane of a 5–20% SDS-PAGE gel with 160 μg protein for nerve tissue and 80 μg protein for muscle (both from the supernatant fraction). This was transferred to Hybond-P membranes (Amersham Pharmacia Biotech) in a transfer buffer of 25 mM Tris, 192 mM glycine, 0.1% SDS and 10% methanol. After immunoprobing with N-20, a rabbit antibody to the androgen receptor (1:1,000 dilution; Santa Cruz Biotechnology), we did secondary antibody probing and detection with the ECL Plus kit (Amersham Pharmacia Biotech). We quantified the signal intensity of the bands smearing from the top of the gel using the NIH Image program (NIH Image version 1.62). The quantitative data of three independent western blots were expressed as mean ± s.d. We reprobed membranes with antibody to α-tubulin (1:5,000 dilution; Santa Cruz Biotechnology). We extracted nuclear and cytoplasmic fractions with NE-PER nuclear and cytoplasmic extraction reagents (Pierce). We reprobed membranes of fractionated western blot with antibody to α-tubulin (1:5,000 dilution and antibody to histone H3 (1:400 dilution; Upstate Biotechnology).

Immunohistochemistry and muscle histology. We perfused 20 ml of a 4% paraformaldehyde fixative in phosphate buffer (pH 7.4) through the left cardiac ventricles of mice deeply anesthetized with ketamine-xylazine, postfixed the tissues overnight in 10% phosphate-buffered formalin, and processed them for paraffin embedding. Then we deparaffinized tissue sections 4 μm in thickness, dehydrated them with alcohol, treated them with formic acid for 5 min at room temperature and stained them with 1C2 (1:10,000 dilution; Chemicon), as described before[15,37,39]. After formalin fixation, we washed tail specimens with 70% ethanol and decalcified them with 7% formic acid and 70% ethanol for 7 d followed by paraffin embedding. To assess 1C2-positive cells in muscle, we calculated the number of 1C2-positive cells in more than 500 fibers in the entire area and expressed the results as the number per 100 muscle fibers. We air-dried cryostat sections (6 μm in thickness) of gastrocnemius muscles and stained them with H&E.

Statistical analysis. We analyzed data using the unpaired *t*-test and considered *P* values ≤0.05 to be statistically significant.

1. Kennedy, W.R., Alter, M. & Sung, J.H. Progressive proximal spinal and bulbar muscular atrophy of late onset. A sex-linked recessive trait. *Neurology* **18**, 671–680 (1968).
2. Sobue, G. *et al.* X-linked recessive bulbospinal neuronopathy. A clinicopathological study. *Brain* **112**, 209–232 (1989).
3. Sobue, G. *et al.* Subclinical phenotypic expressions in heterozygous females of X-linked recessive bulbospinal neuronopathy. *J. Neurol. Sci.* **117**, 74–78 (1993).
4. Mariotti, C. *et al.* Phenotypic manifestations associated with CAG-repeat expansion in the androgen receptor gene in male patients and heterozygous females: a clinical and molecular study of 30 families. *Neuromuscul. Disord.* **10**, 391–397 (2000).
5. Schmidt, B.J., Greenberg, C.R., Allingham-Hawkins, D.J. & Spriggsm E.L. Expression of X-linked bulbospinal muscular atrophy (Kennedy disease) in two homozygous women. *Neurology* **59**, 770–772 (2002).
6. La Spada, A.R., Wilson, E.M., Lubahn, D.B., Harding, A.E. & Fischbeck, K.H. Androgen receptor gene mutations in X-linked spinal and bulbar muscular atrophy. *Nature* **352**, 77–79 (1991).
7. Tanaka, F. *et al.* Founder effect in spinal and bulbar muscular atrophy (SBMA). *Hum. Mol. Genet.* **5**, 1253-1257 (1996).
8. Doyu, M. *et al.* Severity of X-linked recessive bulbospinal neuronopathy correlates with size of the tandem CAG repeat in androgen receptor gene. *Ann. Neurol.* **32**, 707–710 (1992).
9. Igarashi, S. *et al.* Strong correlation between the number of CAG repeats in androgen receptor genes and the clinical onset of features of spinal and bulbar muscular atrophy. *Neurology* **42**, 2300–2302 (1992).
10. Zoghbi, H.Y. & Orr, H.T. Glutamine repeats and neurodegeneration. *Annu. Rev. Neurosci.* **23**, 217–247 (2000).
11. Li, M. *et al.* Nuclear inclusions of the androgen receptor protein in spinal and bulbar muscular atrophy. *Ann. Neurol.* **44**, 249–254 (1998).
12. Li, M. *et al.* Nonneural nuclear inclusions of androgen receptor protein in spinal and bulbar muscular atrophy. *Am. J. Pathol.* **153**, 695–701 (1998).
13. Ross, C.A. Polyglutamine pathogenesis: emergence of unifying mechanisms for Huntington's disease and related disorders. *Neuron* **35**, 819–822 (2002).
14. Taylor, J.P. & Fischbeck, K.H. Altered acetylation in polyglutamine disease: an opportunity for therapeutic intervention? *Trends Mol. Med.* **8**, 195–197 (2002).
15. Katsuno, M. *et al.* Testosterone reduction prevents phenotypic expression in a transgenic mouse model of spinal and bulbar muscular atrophy. *Neuron* **35**, 843–854 (2002).
16. Huggins, C. & Hodges, C.V. Studies on prostatic cancer. I. The effects of castration, of estrogen and of androgen injection on serum phosphates in metastatic carcinoma of the prostate. *Cancer Res.* **1**, 293–297 (1941).
17. Labrie, F. Mechanism of action and pure antiandrogenic properties of flutamide. *Cancer* **72** (suppl. 12), 3816–3827 (1993).
18. Yamamoto, A., Lucas, J.J. & Hen R. Reversal of neuropathology and motor dysfunction in a conditional model of Huntington's disease. *Cell* **101**, 57–66 (2000).
19. Kemppainen, J.A. & Wilson, E.M. Agonist and antagonist activities of hydroxyflutamide and casodex relate to androgen receptor stabilization. *Urology* **48**, 157–163 (1996).
20. Lu, S., Simon, N.G., Wang, Y. & Hu, S. Neural androgen receptor regulation: effects of androgen and antiandrogen. *J. Neurobiol.* **41**, 505–512 (1999).
21. Tomura, A. *et al.* The subnuclear three-dimensional image analysis of androgen receptor fused to green fluorescence protein. *J. Biol. Chem.* **276**, 28395–28401 (2001).
22. Walcott, J.L. & Merry, D.E. Ligand promotes intranuclear inclusions in a novel cell model of spinal and bulbar muscular atrophy. *J. Biol. Chem.* **277**, 50855–50859 (2002).
23. Takeyama, K. *et al.* Androgen-dependent neurodegeneration by polyglutamine-expanded human androgen receptor in *Drosophila*. *Neuron* **35**, 855–864 (2002).
24. Fischbeck, K.H., Lieberman, A., Bailey, C.K., Abel, A. & Merry, D.E. Androgen receptor mutation in Kennedy's disease. *Philos. Trans. R. Soc. Lond. B. Biol. Sci.* **354**, 1075–1078 (1999).
25. Lieberman, A.P., Harmison, G., Strand, A.D., Olson, J.M. & Fischbeck, K.H. Altered transcriptional regulation in cells expressing the expanded polyglutamine androgen receptor. *Hum. Mol. Genet.* **11**, 1967–1976 (2002).
26. Gottlieb, .B, Pinsky, L., Beitel, L.K. & Trifiro, M. Androgen insensitivity. *Am. J. Med. Genet.* **89**, 210–217 (1999).
27. MacLean, H.E., Warne, G.L. & Zajac, J.D. Defects of androgen receptor function: from sex reversal to motor neurone disease. *Mol. Cell. Endocrinol.* **112**, 133–141 (1995).
28. Kobayashi, Y. *et al.* Chaperones Hsp70 and Hsp40 suppress aggregate formation and apoptosis in cultured neuronal cells expressing truncated androgen receptor protein with expanded polyglutamine tract. *J. Biol. Chem.* **275**, 8772–8778 (2000).
29. Adachi, H *et al.* HSP70 chaperone over-expression ameliorates phenotypes of the SBMA transgenic mouse model by reducing nuclear-localized mutant AR protein. *J. Neurosci.* **23**, 2203–2211 (2003).
30. Cummings, C..J, *et al.* Chaperone suppression of aggregation and altered subcellular proteasome localization imply protein misfolding in SCA1. *Nat. Genet.* **19**, 148–154 (1998).
31. Cummings, C.J. *et al.* Over-expression of inducible HSP70 chaperone suppresses neuropathology and improves motor function in SCA1 mice. *Hum. Mol. Genet.* **10**, 1511–1518 (2001).
32. McCampbell, A. *et al.* Histone deacetylase inhibitors reduce polyglutamine toxicity. *Proc. Natl. Acad. Sci. USA* **98**, 15179–15184 (2001).
33. Steffan, J.S. *et al.* Histone deacetylase inhibitors arrest polyglutamine-dependent neurodegeneration in *Drosophila*. *Nature* **413**, 739–743 (2001).
34. Hockly, E. *et al.* Suberoylanilide hydroxamic acid, a histone deacetylase inhibitor, ameliorates motor deficits in a mouse model of Huntington's disease. *Proc. Natl. Acad. Sci. USA* **100**, 2041–2046 (2003).
35. Kobayashi, Y. *et al.* Caspase-3 cleaves the expanded androgen receptor protein of spinal and bulbar muscular atrophy in a polyglutamine repeat length-dependent manner. *Biochem. Biophys. Res. Commun.* **252**, 145–150 (1998).
36. Niwa, H., Yamamura, K. & Miyazaki, J. Efficient selection for high-expression transfectants with a novel eukaryotic vector. *Gene* **108**, 193–199 (1991).
37. Adachi, H. *et al.* Transgenic mice with an expanded CAG repeat controlled by the human AR promoter show polyglutamine nuclear inclusions and neuronal dysfunction without neuronal cell death. *Hum. Mol. Genet.* **10**, 1039–1048 (2001).
38. Luo, S. *et al.* Daily dosing with flutamide or Casodex exerts maximal antiandrogenic activity. *Urology* **50**, 913–919 (1997).
39. Trottier, Y. *et al.* Polyglutamine expansion as a pathological epitope in Huntington's disease and four dominant cerebellar ataxias. *Nature* **378**, 403–406 (1995).

Dorfin Localizes to Lewy Bodies and Ubiquitylates Synphilin-1*

Takashi Ito, Jun-ichi Niwa‡, Nozomi Hishikawa, Shinsuke Ishigaki, Manabu Doyu, and Gen Sobue§

From the Department of Neurology, Nagoya University Graduate School of Medicine, Showa-ku, Nagoya 466-8550, Japan

Parkinson's disease (PD) is a neurodegenerative disease characterized by loss of nigra dopaminergic neurons. Lewy bodies (LBs) are a characteristic neuronal inclusion in PD brains. In this study, we report that Dorfin, a RING finger-type ubiquityl ligase for mutant superoxide dismutase-1, was localized with ubiquitin in LBs. Recently, synphilin-1 was identified to associate with α-synuclein and to be a major component of LBs. We found that overexpression of synphilin-1 in cultured cells led to the formation of large juxtanuclear inclusions, but showed no cytotoxicity. Dorfin colocalized in these large inclusions with ubiquitin and proteasomal components. In contrast to full-length synphilin-1, overexpression of the central portion of synphilin-1, including ankyrin-like repeats, a coiled-coil domain, and an ATP/GTP-binding domain, predominantly led to the formation of small punctate aggregates scattered throughout the cytoplasm and showed cytotoxic effects. Dorfin and ubiquitin did not localize in these small aggregates. Overexpression of the N or C terminus of synphilin-1 did not lead to the formation of any aggregates. Dorfin physically bound and ubiquitylated synphilin-1 through its central portion, but did not ubiquitylate wild-type or mutant α-synuclein. These results suggest that the central domain of synphilin-1 has an important role in the formation of aggregates and cytotoxicity and that Dorfin may be involved in the pathogenic process of PD and LB formation by ubiquitylation of synphilin-1.

Parkinson's disease (PD)[1] is a neurodegenerative disease caused by loss of nigra dopaminergic neurons. Lewy bodies (LBs) are a characteristic neuronal inclusion in PD brains (1–4). Although LBs are a prominent pathological feature of PD, the underlying molecular mechanism accounting for LB formation is poorly understood. Several lines of evidence have suggested that derangements in the ubiquitin/proteasome pro-

‡ Research Fellow of the Japan Society for the Promotion of Science for Young Scientists.

§ To whom correspondence should be addressed: Dept. of Neurology, Nagoya University Graduate School of Medicine, 65 Tsurumai-cho, Showa-ku, Nagoya 466-8550, Japan. Tel.: 81-52-744-2385; Fax: 81-52-744-2384; E-mail: sobueg@med.nagoya-u.ac.jp.

[1] The abbreviations used are: PD, Parkinson's disease; LBs, Lewy bodies; E1, ubiquitin-activating enzyme; E2, ubiquitin carrier protein; E3, ubiquitin-protein isopeptide ligase; HEK293, human embryonic kidney 293; ALS, amyotrophic lateral sclerosis; SOD1, superoxide dismutase-1; IP, immunopurified; MTS, 3-(4,5-dimethylthiazol-2-yl)-5-(3-carboxymethoxyphenyl)-2-(4-sulfophenyl)-2H-tetrazolium, inner salt.

tein degradation pathway play a prominent role in the pathogenesis of PD (5). Ubiquitin and proteasome subunits colocalize in LBs (6, 7), and biochemical studies have revealed reduced catalytic activities of proteasomes in the lesions of PD (8, 9). The gene product responsible for autosomal recessive juvenile parkinsonism, parkin (10), is an E3 ubiquityl ligase (11–13). Accumulation of target protein(s) due to loss of the ubiquitylation function of parkin may contribute to the development of autosomal recessive juvenile parkinsonism. In addition, a missense mutation in UCHL1 (ubiquitin C-terminal hydrolase L1) has been described in a family with PD (14). UCHL1 produces monomeric ubiquitin by cleaving polyubiquitin chains (15). Recently, ubiquityl ligase activity as well as the hydrolase activity of UCHL1 were also reported (16).

α-Synuclein is a 19-kDa presynaptic vesicular protein of unconfirmed function and one of the major components of LBs (17, 18). Mutations in α-synuclein (A30P and A53T) cause a rare autosomal dominant form of PD, which shares many phenotypic characteristics with sporadic PD (19, 20). α-Synuclein aggregates deposit in LBs in both autosomal dominant and sporadic forms of PD (21, 22). In addition, it has been reported that transgenic flies and mice overexpressing human wild-type or mutant α-synuclein have abnormal cellular accumulation of α-synuclein and neuronal dysfunction and degeneration (23–30), indicating that α-synuclein has a role in the pathogenesis of both familial and sporadic forms of PD.

Synphilin-1 was identified recently by yeast two-hybrid techniques as a novel protein that interacts with α-synuclein (31). α-Synuclein amino acids 1–65 are is sufficient for interaction, and the central portion of synphilin-1 (amino acids 349–555) is necessary and sufficient for interaction with α-synuclein (32). It has also been reported that the C terminus of α-synuclein is closely associated with the C terminus of synphilin-1 and that a weak interaction occurs between the N terminus of α-synuclein and synphilin-1 (33). Synphilin-1 is highly concentrated in presynaptic nerve terminals, and its association with synaptic vesicles is modulated by α-synuclein (34). Coexpression of α-synuclein and synphilin-1 in transfected cells results in the formation of eosinophil cytoplasmic inclusions that resemble LBs (31, 35), whereas transfection of synphilin-1 alone without expression of α-synuclein or parkin can also produce cytoplasmic inclusions in cultured cells (36, 37). Furthermore, synphilin-1 is ubiquitylated and degraded by proteasomes in human embryonic kidney 293 (HEK293) cells (37) and is localized as another major component of LBs in the brains of patients with PD (38, 39). Thus, the process through which aggregations are formed by synphilin-1 may be important in the pathogenesis of PD.

Dorfin is a gene product (which we cloned from anterior horn tissues of human spinal cord) (40) that contains a RING finger/IBR (in between RING finger) motif (41) at its N terminus. It was reported that HHARI (human homologue of ariadne) and H7-AP1 (UbcH7-associated protein-1), both RING finger/IBR
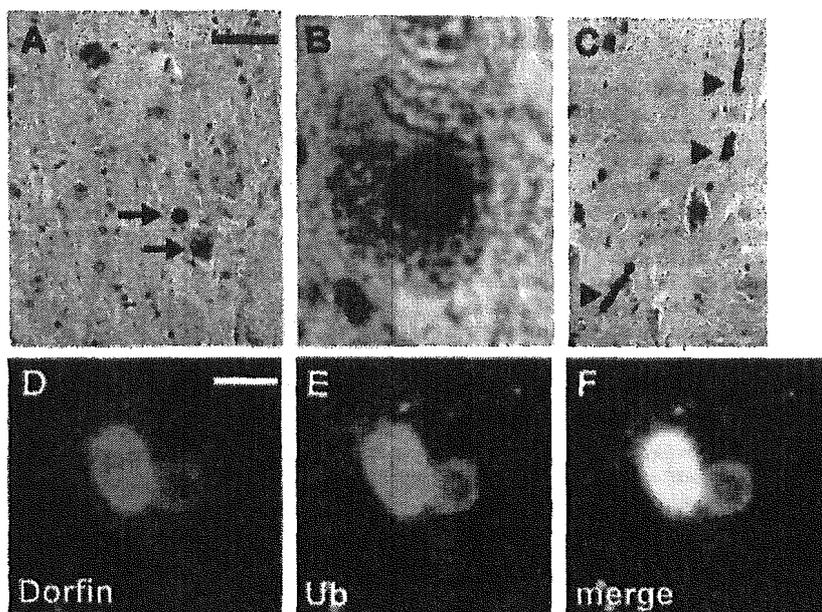
Fig. 1. **Colocalization of Dorfin and ubiquitin in LBs of PD.** Substantia nigra tissue of PD cases was immunohistochemically stained with anti-Dorfin antibody. *A*, LBs (*arrows*) in neurons were strongly stained. *B*, the peripheral rim of a typical LB was predominantly stained with anti-Dorfin antibody. *C*, Lewy neurites (*arrowheads*) were also Dorfin-immunoreactive. The *scale bar* in *A* is equivalent to 100 μm in *A* and *C* and 12 μm in *B*. *D–F*, shown are laser scanning confocal microscopy images of double-labeling immunofluorescence study of LB. Frozen sections prepared from substantia nigra tissue of PD were incubated with rabbit anti-Dorfin IgG and labeled with Alexa Fluor 568-conjugated anti-rabbit antibodies (*red* in *D*) and mouse monoclonal anti-ubiquitin and Alexa Fluor 488-conjugated anti-mouse antibodies (*green* in *E*). *F* shows a merged image of the double-stained LB (*D* and *E*), and regions of overlap between Dorfin and ubiquitin immunoreactivities are shown in *yellow*. The *scale bar* in *D* is equivalent to 10 μm and also applies to *E* and *F*.

motif-containing proteins, interact with the ubiquitin carrier protein (E2) UbcH7 through the RING finger/IBR motif and that a distinct subclass of RING finger/IBR motif-containing proteins represents a new family of proteins that specifically interact with distinct E2 enzymes (42, 43). Dorfin is a juxtanuclearly located E3 ubiquityl ligase and may function in the microtubule-organizing centers (40). In the spinal cords of patients with sporadic and familial forms of amyotrophic lateral sclerosis (ALS) with an SOD1 mutation, Dorfin is colocalized with ubiquitin in hyaline inclusions (44). Dorfin physically binds and ubiquitylates various SOD1 mutants derived from familial ALS patients and enhances their degradation (44). Thus, an important and interesting question is whether Dorfin is colocalized with ubiquitin in LBs of PD.

In this study, we show that Dorfin is colocalized with ubiquitin in LBs of PD. We found that Dorfin ubiquitylates synphilin-1 and that overexpression of synphilin-1 leads to ubiquitylated inclusions resembling LBs in cultured cells.

EXPERIMENTAL PROCEDURES

Immunohistochemistry—Immunohistochemical studies were carried out on 20% buffered, Formalin-fixed, paraffin-embedded autopsied brains filed in the Department of Neurology of the Nagoya University Graduate School of Medicine. Five PD brains (67–69 years of age, four men and one woman) and five controls without neurological disease (61–78 years of age, four men and one woman) were studied. The diagnosis of all cases was confirmed by clinical and pathological criteria. Immunohistochemistry was performed as described previously (45). Rabbit polyclonal antiserum was raised against a C-terminal portion of Dorfin (amino acid 678–690) as described previously (40). Dorfin antiserum (1:200 dilution) and monoclonal anti-ubiquitin antibody (P4D1, 1:400 dilution; Santa Cruz Biotechnology) were used. To assess the colocalization of Dorfin and ubiquitin, a double-labeling immunofluorescence study was performed on selected sections with a combination of anti-Dorfin and anti-ubiquitin antibodies. Anti-Dorfin antibody was visualized by goat anti-rabbit IgG coupled with Alexa Fluor 568 (Molecular Probes, Inc.), and anti-ubiquitin antibody was visualized with sheep anti-mouse IgG coupled with Alexa Fluor 488 (Molecular Probes, Inc.) and observed under a Carl Zeiss LSM-510 laser scanning confocal microscope. For cultured cells, immunostaining was performed as fol-

lows. COS-7 cells transiently expressing synphilin-1-DsRed fusion protein in a 4-chamber slide (Nalge Nunc) coated with rat tail collagen (Roche Diagnostics) were fixed with methanol at −20 °C for 10 min, air-dried, and blocked with 5% goat serum for 30 min. Cells were then incubated overnight at 4 °C with the appropriate primary antibody diluted in phosphate-buffered saline. After washing three times with phosphate-buffered saline, Alexa Fluor 488-conjugated secondary antibody (1:1000 dilution; Molecular Probes, Inc.) was added for 1 h at room temperature. Samples were visualized under an Olympus BX51 epifluorescence microscope. Primary antibodies against ubiquitin (P4D1, 1:200 dilution), Hsp70 (heat shock protein of 70 kDa; 1:5000 dilution; Stressgen Biotech Corp.), the 20 S proteasome core subunit (1:5000 dilution; Affiniti), and UbcH7 (1:100 dilution; Transduction Laboratories) were used.

Expression Plasmids, Cell Culture, and Transfection—Human synphilin-1 cDNA containing the entire coding region was amplified by *Pfu* Turbo DNA polymerase (Stratagene) from human brain cDNAs using 5'-GTCAGGATCCACCACCATGGAAGCCCCTGAATACC-3' as the forward primer and 5'-ATATCTCGAGTGCTGCCTTATTCTTTCCTTT-G-3' as the reverse primer and inserted in-frame into the *Bam*HI and *Xho*I sites of the pcDNA3.1/V5His vector (Invitrogen). A plasmid for DsRed-tagged synphilin-1 was constructed by PCR amplification using 5'-ATATCTCGAGACCACCATGGAAGCCCCTGAATACC-3' as the forward primer and 5'-GTCAGGATCCGCCTTTGCCTTATTCTTTCCT-TTG-3' as the reverse primer and inserted in-frame into the *Xho*I and *Bam*HI sites of the pDsRed-N1 vector (Clontech). A series of deletion mutants of synphilin-1 were prepared as synphilin-1-N (amino acid 1–348), synphilin-1-M (amino acid 349–555), and synphilin-1-C (amino acid 556–919). Synphilin-1-M is the central portion of synphilin-1, containing the ankyrin-like repeat, the coiled-coil domain, and the ATP/GTP-binding domain (31). Primers pairs for each deletion mutant were as follows: 5'-GTCAGGATCCACCACCATGGAAGCCCCTGAAT-ACC-3' and 5'-ATATCTCGAGTTCGTCGTGAATTTTGTCT-3' for synphilin-1-N-V5, 5'-ATATCTCGAGACCACCATGGAAGCCCCTGAA-TACC-3' and 5'-GTCAGGATCCGCTTCGTCGTGAATTTTGTCTAG-3' for synphilin-1-N-DsRed, 5'-GTCAGGATCCACCATGAATGGAAACA-ATCTAT-3' and 5'-ATATCTCGAGCTTGCCCTCTGATTTCTGG-3' for synphilin-1-M-V5, 5'-ATATCTCGAGACCACCATGAATGGAAACAAT-CTAT-3' and 5'-GTCAGGATCCGCC TTGCCCTCTGATTTCTGGGC-3 for synphilin-1-M-DsRed, 5'-GTCAGGATCCACCACCATGTCACTCC-CTTCTTCAC-3' and 5'-ATATCTCGAGTGCTGCCTTATTCTTTCCTT-TG-3' for synphilin-1-C-V5, and 5'-ATATCTCGAGACCACCATGTCA-CTCCCTTCTTCAC-3' and 5'-GTCAGGATCCGCCTTTGCCTTATTCT-

TTCCTTTG-3' for synphilin-1-C-DsRed. Construction of pcDNA4/His-Max-Dorfin, pcDNA3.1(+)FLAG-ubiquitin, and pcDNA3.1/MycHis(+)-SOD1 vectors was described elsewhere (40, 44). α-Synuclein cDNA was amplified by PCR from human brain cDNAs and cloned into the *Eco*RV site of pcDNA3.1/MycHis(+) (Invitrogen). To generate the mutant α-synuclein expression vector, A30P and A53T mutations were introduced into pcDNA3.1/MycHis(+)-α-synuclein with a QuikChange site-directed mutagenesis kit (Stratagene) following the method of Lee *et al.* (46). COS-7, HEK293, and Neuro2a cells were maintained in Dulbecco's modified Eagle's medium with 10% fetal calf serum. Transfections were performed using the Effectene transfection reagent (QIAGEN Inc.) according to the manufacturer's instructions. To inhibit cellular proteasome activity, cells were treated with 0.5 μM MG132 (carbobenzoxy-L-leucyl-L-leucyl-L-leucinal, Sigma) for 16 h overnight after transfection.

*Immunoprecipitation and Western Blot Analysis*—Cells were lysed in lysis buffer (50 mM Tris, 150 mM NaCl, 1% Nonidet P-40, and 0.1% SDS) with Complete protease inhibitor mixture (Roche Diagnostics). Immunoprecipitation from transfected cell lysates was performed with 2 μg of antibody and protein A/G Plus-agarose (Santa Cruz Biotechnology), and the immunoprecipitate was then washed four times with lysis buffer. Anti-V5 antibody (Invitrogen) for synphilin-1-V5 fusion proteins and anti-Myc antibody (A-14, Santa Cruz Biotechnology) for α-synuclein-Myc or SOD1-Myc fusion proteins were used. Immunoprecipitates were subjected to SDS-PAGE and analyzed by Western blotting with ECL detection reagents (Amersham Biosciences).

In Vitro Ubiquitylation Assay—Immunopurified (IP) Xpress-Dorfin bound to anti-Xpress antibody (Invitrogen) with protein A/G Plus-agarose (Santa Cruz Biotechnology) was prepared from lysates of HEK293 cells transfected with pcDNA4/HisMax-Dorfin. IP-synphilin-1-V5 was prepared with anti-V5 antibody bound to protein A/G Plus-agarose from lysates of HEK293 cells transfected with pcDNA3.1/V5His-synphilin-1. IP-α-synuclein-Myc and IP-SOD1-Myc were prepared with anti-Myc antibodies from lysates of pcDNA3.1/MycHis(+)-α-synuclein- and pcDNA3.1/MycHis(+)-SOD1-transfected HEK293 cells, respectively. Slurries of IP-Xpress-Dorfin were mixed with IP-synphilin-1-V5, IP-α-synuclein-Myc, or IP-SOD1-Myc and incubated at 30 °C for 90 min in 50 μl of reaction buffer containing ATP (4 mM ATP in 50 mM Tris-HCl (pH 7.5), 2 mM MgCl₂, and 2 mM dithiothreitol), 100 ng of rabbit E1 (Calbiochem), 2 μg of UbcH7 (Affiniti), and 2 μg of His-ubiquitin (Calbiochem). The reaction was terminated by adding 20 μl of 4× sample buffer, and 20-μl aliquots of the reaction mixtures were subjected to SDS-PAGE, followed by Western blotting with anti-His antibody (Novagen).

Neurotoxicity Analysis and Quantification of Synphilin-1 Aggregates—COS-7 cells (1 × 10⁴) were grown overnight on collagen-coated 4-chamber well slides. They were transfected with 0.2 μg of pDsRed-N1-synphilin-1 or its deletion mutants. To inhibit cellular proteasome activity, cells were treated with 0.5 μM MG132 for 16 h overnight after transfection. The number of inclusions was counted in >100 cells randomly selected, and data were averaged from three independent experiments. For cell viability assay, 5 × 10³ Neuro2a cells were grown in collagen-coated 96-well plates overnight. They were then transfected with 0.1 μg of pcDNA3.1/V5His-synphilin-1 or deletion mutants of synphilin-1. pcDNA3.1/V5His-LacZ was used as a control. Next, an MTS-based cell proliferation assay was performed using CellTiter 96 (Promega) at 24 h after serum deprivation. The assay was carried out in triplicate. Absorbance at 490 nm was measured in a multiple plate reader.
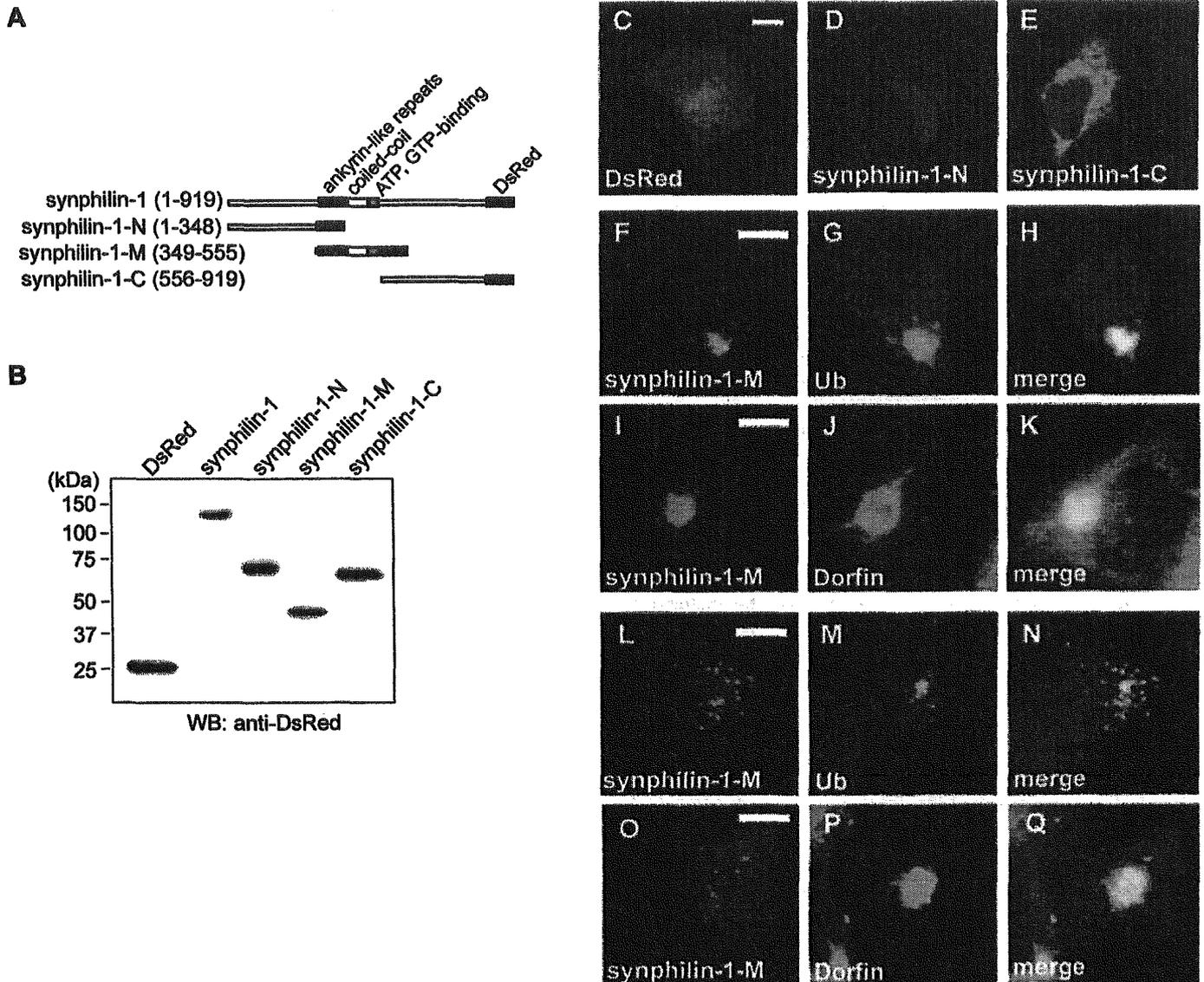
RESULTS

Dorfin Localizes to LBs of PD—We first examined whether LBs contain Dorfin. Immunohistochemical analysis revealed that Dorfin was predominantly localized in LBs found in PD (Fig. 1A). The peripheral rim of a typical LB in a neuronal cell body was strongly stained, whereas the central core remained unstained (Fig. 1B). Dorfin was also localized in Lewy neurites (Fig. 1C), which are a pathological hallmark in addition to LBs of degenerating neurons in the brains of patients suffering from PD (47). Anti-Dorfin antibody did not stain any abnormal structures in normal brains (data not shown). A double-labeling immunofluorescence study revealed that Dorfin was colocalized with ubiquitin in LBs (Fig. 1, D–F). Serial sections stained with anti-Dorfin and anti-ubiquitin antibodies showed that ~90% of ubiquitylated LBs were positive for Dorfin immunoreactivity. The staining profile of Dorfin was very similar
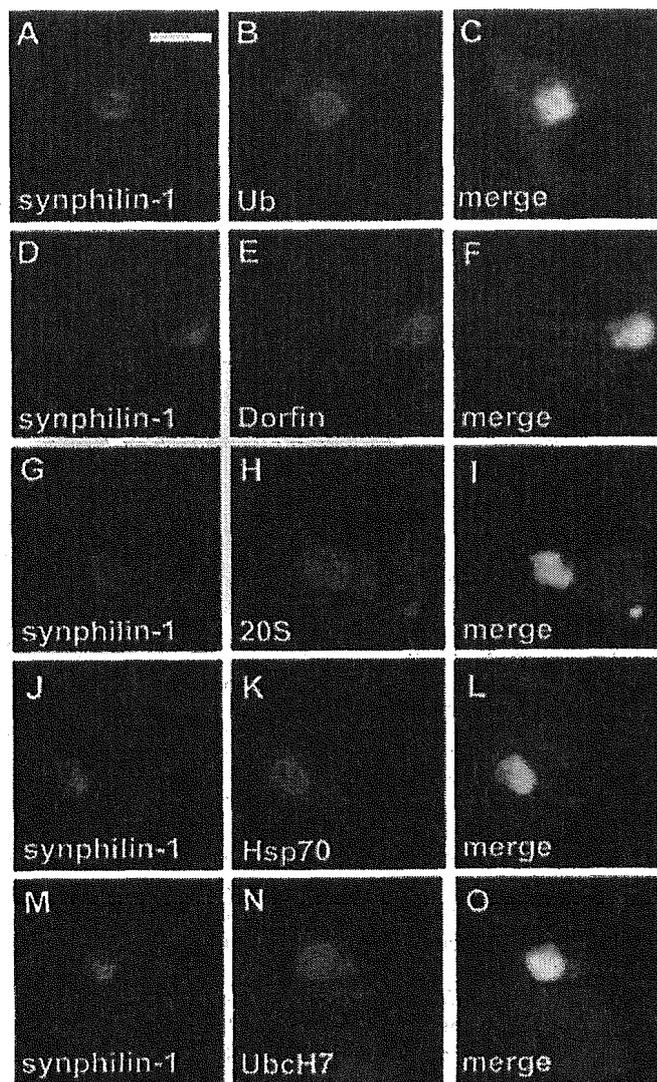
FIG. 2. **Formation of large juxtanuclear inclusions by overexpression of synphilin-1.** Full-length synphilin-1 was overexpressed in COS-7 cells as DsRed fusion protein. Two days after transfection, cells were fixed and immunostained with the indicated antibodies. Large juxtanuclear inclusions of synphilin-1 were formed spontaneously without proteasome inhibition. Cells with large juxtanuclear inclusions were co-stained with ubiquitin (*Ub*) (*A–C*), Dorfin (*D–F*), 20 S proteasome core subunit (*G–I*), Hsp70 (*J–L*), or UbcH7 (*M–O*). Regions of overlap between synphilin-1 (*red*) and immunoreactivities of the indicated proteins (*green*) are shown in *yellow*. Nuclei were stained with Hoechst 33342 (*blue*). *Scale bar* = 10 μm.

to that of α-synuclein (48), which is predominantly located in the peripheral rim of LBs, but was different from that of parkin, which localizes predominantly in the core of LBs (49).

Expression of Synphilin-1 Induces LB-like Large Juxtanuclear Inclusions, and Dorfin Localizes to These Inclusions—To investigate the relationships of Dorfin to components of LBs other than ubiquitin, we first examined the subcellular localization of α-synuclein and synphilin-1 in cultured cells. We created wild-type and mutant α-synuclein-green fluorescent protein and α-synuclein-Myc fusion constructs, but there was no evidence of α-synuclein aggregation in transfected COS-7 cells in the presence or absence of the proteasome inhibitor (data not shown). We created a synphilin-1-DsRed fusion construct by fusing the red fluorescent protein DsRed to the C terminus of synphilin-1 and carried out transient transfection in COS-7 cells with this construct. Large juxtanuclear inclusions were spontaneously formed in the transfected COS-7 cells in the absence of the proteasome inhibitor (Fig. 2, A–O). We

A

synphilin-1 (1-919)
synphilin-1-N (1-348)
synphilin-1-M (349-555)
synphilin-1-C (556-919)

B

(kDa)
150 -
100 -
75 -
50 -
37 -
25 -

WB: anti-DsRed

FIG. 3. **Formation of two types of aggregates by the central portion of synphilin-1.** COS-7 cells were transfected with expression vectors for DsRed alone or DsRed fusion proteins of synphilin-1 deletion mutants. Two days after transfection, cells were analyzed by Western blotting (*WB*) and immunocytochemistry. Shown are a schematic representation of the DsRed fusion proteins of synphilin-1 deletion mutants used in this study (*A*) and the results from Western blot analysis of lysates from transfected cells (*B*). DsRed alone (*C*), synphilin-1-N (*D*), and synphilin-1-C (*E*) formed no aggregates, whereas overexpression of the central portion of synphilin-1 (synphilin-1-M) induced two types of inclusions: large juxtanuclear inclusions (*F* and *I*) and small punctate aggregates scattered throughout the cytoplasm (*L* and *O*). Large juxtanuclear inclusions were ubiquitin (*Ub*)-positive (*F–H*) and colocalized with Dorfin (*I–K*), whereas small punctate aggregates were ubiquitin-negative (*L–N*) and did not colocalize with Dorfin (*O–Q*). Regions of overlap between synphilin-1 (*red*) and immunoreactivities of the indicated proteins (*green*) are shown in *yellow*. Nuclei were stained with Hoechst 33342 (*blue*). *Scale bar* = 10 μm.

also constructed synphilin-1 fusion proteins with a smaller V5/His₆ tag, which formed identical inclusions when overexpressed in COS-7 cells, although to a lesser extent than synphilin-1-DsRed fusion proteins (data not shown). Immunostaining with anti-ubiquitin and anti-Dorfin antibodies revealed that most of the large juxtanuclear inclusions of synphilin-1 contained ubiquitin (Fig. 2, *A–C*) and Dorfin (*D–F*). Immunohistochemical studies of human LBs have previously shown that LBs are stained with proteasome subunits (6) and molecular chaperones such as Hsp40 and Hsp70 (24). Thus, we next examined whether the inclusion bodies in COS-7 cells contain the 20 S proteasome core subunit and Hsp70. We found both the 20 S proteasome subunit and Hsp70 to be colocalized with synphilin-1 inclusion bodies (Fig. 2, *G–L*). Dorfin binds specifically to UbcH7 as an E2 through the RING finger/IBR domain (40). UbcH7 was also localized with Dorfin in these inclusions (Fig. 2, *M–O*). These observations suggest that large

juxtanuclear inclusions formed by synphilin-1 in our cell culture system have many characteristic features of LBs, that synphilin-1 can aggregate when overexpressed, and that this process may be associated with its ubiquitylation.

Expression of the Central Portion of Synphilin-1 Induces Large Juxtanuclear Inclusions as Full-length Proteins, but Small Punctate Aggregates Are Also Formed—To further analyze which part of synphilin-1 is related to aggregation formation, we prepared a series of deletion mutants of synphilin-1. We divided synphilin-1 into three parts, the N terminus of synphilin-1 (synphilin-1-N) containing amino acids 1–348, the central portion of synphilin-1 (synphilin-1-M) containing amino acids 349–555, and the C terminus of synphilin-1 (synphilin-1-C) containing amino acids 556–919, and fused them to DsRed at their C termini (Fig. 3, *A* and *B*). Inclusions were not seen with overexpression of DsRed alone, synphilin-1-N, or synphilin-1-C in COS-7 cells (Fig. 3, *C–E*). However, expression of

synphilin-1-M resulted in the production of two types of inclusions: large juxtanuclear inclusions (Fig. 3, F–K) and small punctate aggregates scattered throughout the cytoplasm (L–Q). The large inclusions were stained with ubiquitin (Fig. 3, F–H) and Dorfin (I–K), as were inclusions induced by full-length synphilin-1. However, neither ubiquitin nor Dorfin was colocalized with the small punctate aggregates scattered throughout the cytoplasm (Fig. 3, L–Q).

Expression of the Central Portion of Synphilin-1 Compromises Cell Viability—We examined the frequency of the inclusion formation by synphilin-1 and its deletion mutants. The number of inclusions was counted with and without the proteasome inhibitor MG132 in COS-7 cells (Fig. 4A). Both synphilin-1-N and synphilin-1-C formed almost no inclusions in either the presence or absence of MG132. Full-length synphilin-1 and synphilin-1-M produced inclusions with high frequency even in the absence of MG132, and the number of cells with inclusions induced by full-length synphilin-1 was significantly greater than that induced by synphilin-1-M (Fig. 4A). Treatment with MG132 significantly increased the number of inclusions. We next measured the ratio of cells that contained small punctate aggregates to total cells bearing all inclusions (Fig. 4B) because two types of aggregates, large juxtanuclear inclusions and small punctate scattered aggregates, were observed. In contrast to full-length synphilin-1, the inclusions induced by overexpression of synphilin-1-M were predominantly small punctate aggregates scattered through the cytoplasm (Fig. 4B). Treatment with MG132 decreased the ratio of small aggregates induced by synphilin-1-M (Fig. 4B).
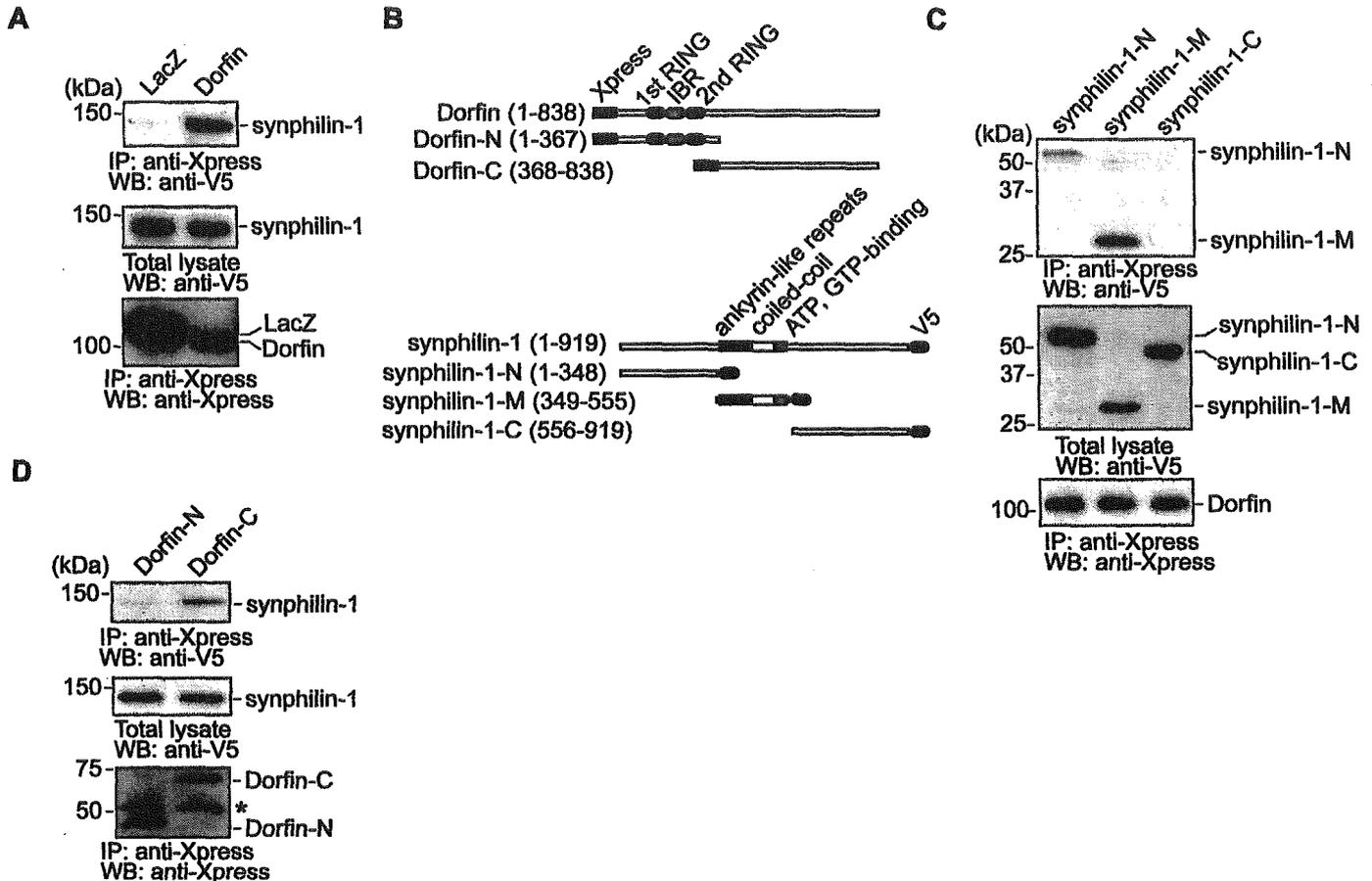
The effects of synphilin-1 expression on cell viability are poorly understood. O'Farrell et al. (36) reported that cells transfected with synphilin-1 are more viable than cells transfected with LacZ. On the other hand, Lee et al. (37) reported that synphilin-1 compromises cell viability. Thus, we examined the effects of synphilin-1 and its deletion mutants on cell viability using the MTS assay in the neuronal cell line Neuro2a (Fig. 4C). We found that synphilin-1-M had a cytotoxic effect, whereas overexpression of full-length synphilin-1 or the N- or C-terminal deletion mutant of synphilin-1 did not (Fig. 4C). We used synphilin-1-V5 fusion constructs, but synphilin-1-DsRed fusion constructs gave the same results (data not shown).

Dorfin Interacts with Synphilin-1—We examined whether Dorfin interacts with synphilin-1 because Dorfin localizes in LBs and cytoplasmic juxtanuclear inclusions formed by synphilin-1. To identify which portion of synphilin-1 binds to Dorfin, we expressed a series of deletion mutants of V5-tagged synphilin-1 and Xpress-tagged Dorfin in COS-7 cells (Fig. 5B). Co-immunoprecipitation confirmed that Dorfin bound to full-length synphilin-1 (Fig. 5A) and interacted strongly with synphilin-1-M and weakly with synphilin-1-N, but Dorfin failed to bind to synphilin-1-C (Fig. 5C). Thus, Dorfin interacts with synphilin-1 mainly through its central portion, which contains the ankyrin-like repeat, the coiled-coil domain, and the ATP/GTP-binding domain. Dorfin has a unique primary structure containing a RING finger/IBR motif at its N terminus and can be structurally divided into two parts, the N-terminal region containing a RING finger/IBR motif (Dorfin-N) that interacts with E2 and the C-terminal region with no similarity to any other known proteins (Dorfin-C) (Fig. 5B) (40). We found that Dorfin-C, but not Dorfin-N, specifically bound synphilin-1, indicating that Dorfin binds to synphilin-1 via its C-terminal region (Fig. 5D).

Dorfin Ubiquitylates Synphilin-1 through Its Central Domain In Vitro—The physical interaction between Dorfin and synphilin-1 prompted us to investigate whether synphilin-1 itself is ubiquitylated by Dorfin. We first examined whether
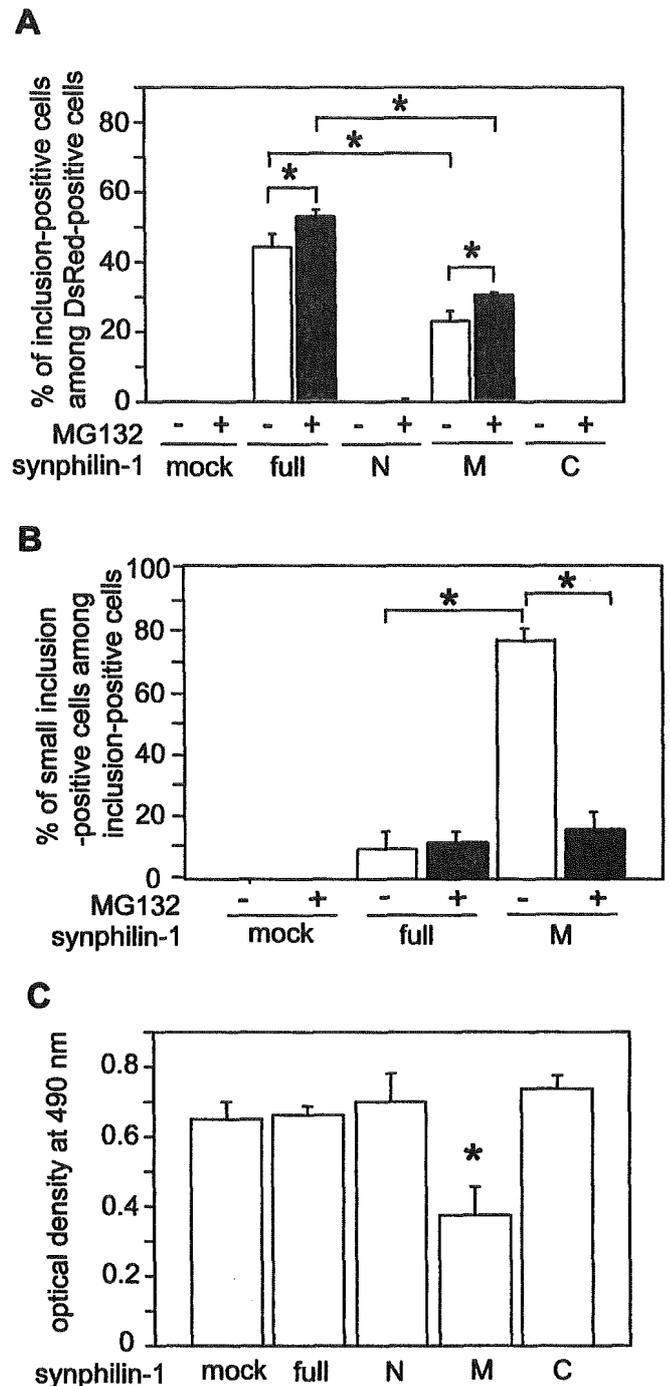
FIG. 4. **The central portion of synphilin-1 produces predominantly small punctate aggregates and compromises cell viability.** A, the frequency of inclusion-bearing cells transfected with synphilin-1 and its deletion mutants. COS-7 cells were grown on collagen-coated 4-chamber well slides and transfected with expression vectors for synphilin-1-DsRed fusion proteins. Two days after transfection, cells were fixed, and percentages of inclusion-positive cells among DsRed-positive cells were determined. For proteasome inhibition, cells were treated with 0.5 μM MG132 for 16 h before fixation. B, the frequency of cells bearing small punctate aggregates scattered through the cytoplasm among all inclusion-positive cells. Experimental conditions were same as described for A. Data are the means ± S.D. of triplicate assays. Statistical analyses were carried out with Mann-Whitney's U test. *, $p < 0.01$. C, the cytotoxic effect of synphilin-1-M expression in an MTS assay. Neuro2a cells were grown on collagen-coated 96-well plates and transfected with V5-tagged synphilin-1 or its deletion mutants. After changing to a serum-free medium, MTS assays were performed after 24 h of incubation. Viability of cells was measured as the level of absorbance at 490 nm. Data are means ± S.D. of triplicate assays. Statistical analyses were carried out by one-way analysis of variance. *, $p < 0.01$.

A

(kDa)
LacZ Dorfin
150- — synphilin-1
IP: anti-Xpress
WB: anti-V5

150- — synphilin-1
Total lysate
WB: anti-V5

100- LacZ
Dorfin
IP: anti-Xpress
WB: anti-Xpress

B

Xpress 1st RING IBR 2nd RING

Dorfin (1-838)
Dorfin-N (1-367)
Dorfin-C (368-838)

ankyrin-like repeats coiled-coil ATP, GTP-binding V5

synphilin-1 (1-919)
synphilin-1-N (1-348)
synphilin-1-M (349-555)
synphilin-1-C (556-919)

C

synphilin-1-N synphilin-1-M synphilin-1-C

(kDa)
50-
37- — synphilin-1-N

25- — synphilin-1-M
IP: anti-Xpress
WB: anti-V5

50- synphilin-1-N
37- synphilin-1-C
— synphilin-1-M
25-
Total lysate
WB: anti-V5

100- — Dorfin
IP: anti-Xpress
WB: anti-Xpress

D

Dorfin-N Dorfin-C
(kDa)
150- — synphilin-1
IP: anti-Xpress
WB: anti-V5

150- — synphilin-1
Total lysate
WB: anti-V5

75- — Dorfin-C
50- * — Dorfin-N
IP: anti-Xpress
WB: anti-Xpress

FIG. 5. **Association of Dorfin with synphilin-1 in COS-7 cells.** A, Dorfin binds to synphilin-1. V5-tagged synphilin-1 or LacZ was cotransfected with Xpress-tagged Dorfin in COS-7 cells. After immunoprecipitation (IP) was performed with anti-Xpress antibody, the resulting precipitates and cell lysate were analyzed by Western blotting (WB) with horseradish peroxidase-conjugated anti-V5 or anti-Xpress antibody. B, schematic representation of Xpress-tagged Dorfin, deletion mutants of Dorfin (i.e. Dorfin-N and Dorfin-C), V5-tagged synphilin-1, and deletion mutants of synphilin-1 (i.e. synphilin-1-N, synphilin-1-M, and synphilin-1-C) used in this study. C, Dorfin binds to synphilin-1 mainly through its central portion. After V5-tagged deletion mutants of synphilin-1 and Xpress-tagged Dorfin were transfected, immunoprecipitation and Western blotting were performed as described for A. D, binding of synphilin-1 to the C-terminal portion of Dorfin. After V5-tagged synphilin-1 and Xpress-tagged deletion mutants of Dorfin were transfected, immunoprecipitation and Western blotting were performed as described for A.
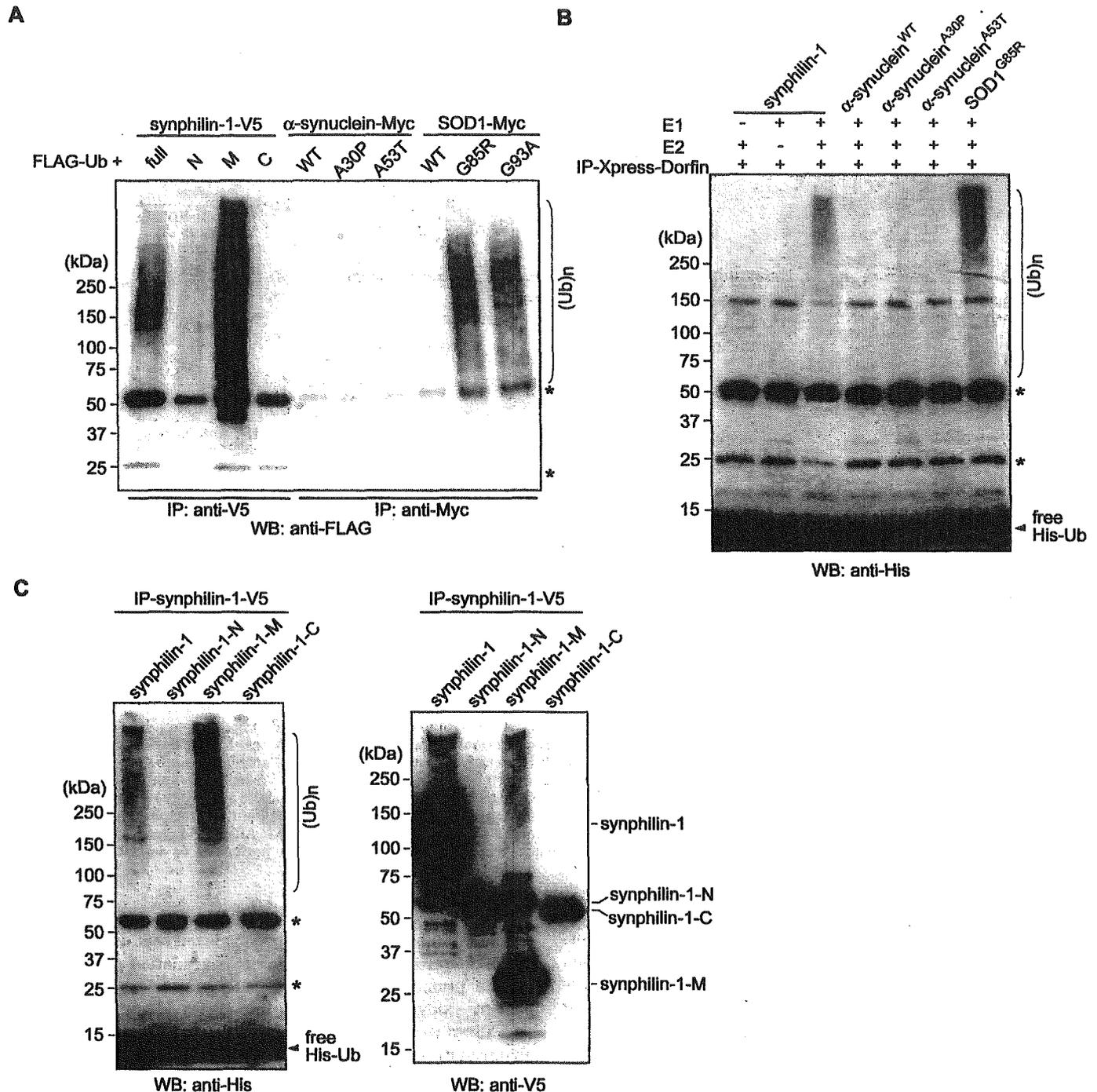
synphilin-1 is ubiquitylated in a culture cell model. V5-tagged full-length synphilin-1 or its deletion mutants were cotransfected with FLAG-tagged ubiquitin in HEK293 cells. When full-length synphilin-1 or its deletion mutants were immunoprecipitated after treatment with the proteasome inhibitor MG132, full-length synphilin-1 and synphilin-1-M were found to be polyubiquitylated, but synphilin-1-N and synphilin-1-C were not (Fig. 6A). Wild-type and mutant α-synuclein were found not to be polyubiquitylated, whereas, as previously reported (44), mutant SOD1 was polyubiquitylated (Fig. 6A).

We next examined whether Dorfin is involved in the ubiquitylation of synphilin-1 in vitro. For this purpose, we immuno-purified Xpress-Dorfin and synphilin-1-V5 independently after transfection into HEK293 cells. When these immunopurified proteins were incubated with recombinant E1, E2 (UbcH7), His-tagged ubiquitin, and ATP, high molecular mass ubiquitylated bands were observed in the presence of Xpress-Dorfin with synphilin-1, whereas no signal was noted with synphilin-1 in the absence of either E1 or E2 (Fig. 6B). Dorfin ubiquitylated mutant SOD1 in vitro, as previously reported (44). Dorfin did not ubiquitylate either wild-type or mutant α-synuclein (Fig. 6B). In vitro ubiquitylation assay of a series of synphilin-1 deletion mutants with Dorfin revealed that synphilin-1-M was ubiquitylated, whereas synphilin-1-N and synphilin-1-C were not ubiquitylated at all (Fig. 6C).

DISCUSSION

Several lines of evidence have suggested that derangements in the ubiquitin-proteasome protein degradation pathway may have a prominent role in the pathogenesis of PD (5). Our present study shows that Dorfin, an E3 ubiquityl ligase, is colocalized with ubiquitin in LBs of PD and physically binds to ubiquitylate synphilin-1, which is known to be a major component of LBs (31, 38, 39).

For the analysis of LB formation by synphilin-1, various cell culture models have been reported (31, 35-37). In our cell culture model, overexpression of synphilin-1 alone induced large juxtanuclear cytoplasmic inclusions. In these large inclusions, Dorfin was colocalized with ubiquitin/proteasome pathway-related proteins such as ubiquitin, the 20 S proteasome core subunit, and Hsp70, just as Dorfin in LBs. The central portion of synphilin-1 contains the ankyrin-like repeat, the coiled-coil domain, and the ATP/GTP-binding domain (31). This region is reported to be necessary for interaction with α-synuclein (32). We found that the central portion of synphilin-1 also bound with Dorfin and that overexpression of this region alone led to inclusion body formation, whereas neither the N- nor C-terminal regions induced aggregates. Overexpression of this central portion of synphilin-1 produced small punctate aggregates scattered throughout the cytoplasm as well as large juxtanuclear inclusions, but the former predominated.

FIG. 6. **Ubiquitylation of synphilin-1 by Dorfin.** *A,* synphilin-1 is ubiquitylated in HEK293 cells. V5-tagged synphilin-1 or its deletion mutants were cotransfected with FLAG-tagged ubiquitin (*Ub*) in HEK293 cells and treated with 0.5 μM MG132 for 16 h overnight after transfection. Myc-tagged α-synuclein or SOD1 was cotransfected with FLAG-ubiquitin and treated as described above. Immunoprecipitates (*IP*) prepared with anti-V5 or anti-Myc antibody were used for immunoblotting with anti-FLAG antibody. *B, in vitro* ubiquitylation assay of synphilin-1 with Dorfin. Xpress-tagged Dorfin and V5-tagged synphilin-1 were transfected into HEK293 cells independently. Immunopurified Dorfin (IP-Xpress-Dorfin) and synphilin-1 (IP-synphilin-1-V5) were prepared and mixed in an assay mixture for ubiquitylation. For this assay, Myc-tagged wild-type (*WT*) and mutant α-synuclein and Myc-tagged mutant SOD1(G85R) were also used instead of synphilin-1. After a 90-min incubation at 30 °C, SDS-PAGE was performed, followed by Western blotting (*WB*) for His-tagged ubiquitin with anti-His antibody. *C, in vitro* ubiquitylation assay of various synphilin-1 deletion mutants with Dorfin. V5-tagged deletion mutants of synphilin-1 were transfected into HEK293 cells, immunopurified, and mixed with IP-Xpress-Dorfin in an assay mixture for ubiquitylation as described for *B.* The reaction products were analyzed by Western blotting with anti-His antibody for ubiquitin (*left panel*) and with anti-V5 antibody for synphilin-1 (*right panel*). High molecular mass ubiquitylated synphilin-1 and synphilin-1-M are shown as (*Ub*)*n. Asterisks* indicate IgG light and heavy chains.

The small punctate aggregates did not colocalize with either ubiquitin or other proteasome pathway-associated proteins and had cytotoxic effects as revealed by MTS assays. Recently, Lee and Lee (50) reported that overexpression of α-synuclein in culture cells produces two distinct types of aggregates: large juxtanuclear inclusions and small punctate aggregates scat-

tered throughout the cytoplasm. The juxtanuclear inclusion bodies are filled with amyloid-like α-synuclein fibrils, whereas the small aggregates contain non-fibrillar spherical aggregates (50). They suggested that these aggregates appear sequentially, with the smallest population appearing first and the fibrillar inclusions last, and that the small spherical aggre-

gates are the cellular equivalents of protofibrils (50). Protofibrils are recognized to be more important in terms of cytotoxicity than mature fibrils in Aβ (51, 52) and α-synuclein (53, 54). In our cell culture model, overexpression of synphilin-1 produced two distinct types of aggregates, very closely resembling two types of α-synuclein aggregates (50). Thus, the small punctate aggregates scattered throughout the cytoplasm induced by the central portion of synphilin-1 might have characteristics similar to those of protofibrils. Our cell culture system will allow detailed characterization of LB formation and cytotoxic processes in further studies.

We reported previously that Dorfin localizes in the inclusion bodies of familial ALS with SOD1 mutations as well as in those of sporadic ALS and ubiquitylates various SOD1 mutants derived from familial ALS patients (44). Based on these findings, it is conceivable that familial and sporadic forms of ALS share a common mechanism involving the dysfunction of the ubiquitin/proteasome pathway, despite having distinct etiological mechanisms. In sporadic ALS, unknown substrate(s) of Dorfin might play a role in the pathogenesis of the disease and accumulate in ubiquitylated inclusion bodies. The following results support the view that Dorfin plays an important role in the formation of LBs of PD: (i) the presence of Dorfin in LBs and large juxtanuclear inclusions of synphilin-1 in our cell culture model, (ii) the parallel distribution patterns of ubiquitin and Dorfin in LBs and inclusion bodies induced by synphilin-1 in cultured cells, and (iii) the E3 function of Dorfin to ubiquitylate synphilin-1. Dorfin did not ubiquitylate either wild-type or mutant α-synuclein; however, our results cannot exclude the possibility that post-translational modification, such as glycosylation (55) or phosphorylation (56, 57), of α-synuclein may be necessary for it to become a substrate for Dorfin because overexpressed α-synuclein was not phosphorylated in our cell culture system (data not shown). The relation between Dorfin and PD shows striking similarities to the relation between Dorfin and ALS. Our findings raise the possibility that PD and ALS are etiologically distinct, but share a biochemically common metabolic pathway through Dorfin, leading to the formation of ubiquitylated inclusion bodies and to neuronal cell degeneration.

Parkin has been shown to have E3 ubiquityl ligase activity (10–12). It was recently demonstrated that an O-glycosylated α-synuclein (55) and synphilin-1 (35) are the substrates of parkin and that parkin localizes to LBs of sporadic PD (49). The link between sporadic and familial forms of PD through α-synuclein, synphilin-1, and parkin sheds new light on underlying common molecular pathogenic mechanisms in PD. What roles, then, do Dorfin and parkin play with respect to each other in the pathogenesis of PD and/or LB formation? Both proteins have a RING finger/IBR domain and E3 ubiquitin ligase activities. Parkin interacts with both α-synuclein (55) and synphilin-1 (35), whereas Dorfin binds and ubiquitylates only synphilin-1. Parkin resides in the core of LBs (49), whereas Dorfin localizes predominantly to the rim. Impaired function of parkin as an E3 ubiquityl ligase is responsible for one of the most common forms of familial PD, autosomal recessive juvenile parkinsonism (9, 10). However, there has been no analysis of whether *Dorfin* gene mutation causes familial PD. Recently, Valente *et al.* (58, 59) identified a locus, *PARK6*, on chromosome 1p35–1p36 that is involved in the autosomal recessive form of parkinsonism. Interestingly, a human paralog of Dorfin (Dj1174N9.1) has been mapped at 1p34.1–1p35.3 (60). Furthermore, Dorfin was identified by a phage display system to be one of the binding proteins with 2-methylnorharman, an analog of the parkinsonism-inducing toxin, 1-methyl-4-phenylpyridinium cation (61). These findings suggest the utility of analyzing Dj1174N9.1 or Dorfin mutation for potential involve-

ment in familial PD. Production of Dorfin knockout mice will also answer the question of whether Dorfin is essential for pathogenesis and/or ubiquitylated inclusion body formation in PD.

REFERENCES

1. Forno, L. S. (*J. Neuropathol. Exp. Neurol.* **55**, 259–27, 1996
2. Gibb, W. R., and Lees, A. J. (1988) *J. Neurol. Neurosurg. Psychiatry* **51**, 745–752
3. Olanow, C. W., and Tatton, W. G. (1999) *Annu. Rev. Neurosci.* **22**, 123–144
4. McKeith, I. G. (2000) *Ann. N. Y. Acad. Sci.* **920**, 1–8
5. McNaught, K. S., Olanow, C. W., Halliwell, B., Isacson, O., and Jenner, P. (2001) *Nat. Rev. Neurosci.* **2**, 589–594
6. Iwatsubo, T., Yamaguchi, H., Fujimuro, M., Yokosawa, H., Ihara, Y., Trojanowski, J. Q., and Lee, V. M. (1996) *Am. J. Pathol.* **148**, 1517–1529
7. Ii, K., Ito, K., Tanaka, K., and Hirano, A. (1997) *J. Neuropathol. Exp. Neurol.* **56**, 125–131
8. McNaught, K. S., and Jenner, P. (2001) *Neurosci. Lett.* **297**, 191–194
9. Furukawa, Y., Vigouroux, S., Wong, H., Guttman, M., Rajput, A. H., Ang, L., Briand, M., Kish, S. J., and Briand, Y. (2002) *Ann. Neurol.* **51**, 779–782
10. Kitada, T., Asakawa, S., Hattori, N., Matsumine, H., Yamamura, Y., Minoshima, S., Yokochi, M., Mizuno, Y., and Shimizu, N. (1998) *Nature* **392**, 605–608
11. Shimura, H., Hattori, N., Kubo, S., Mizuno, Y., Asakawa, S., Minoshima, S., Shimizu, N., Iwai, K., Chiba, T., Tanaka, K., and Suzuki, T. (2000) *Nat. Genet.* **25**, 302–305
12. Imai, Y., Soda, M., and Takahashi, R. (2000) *J. Biol. Chem.* **275**, 35661–35664
13. Zhang, Y., Gao, J., Chung, K. K., Huang, H., Dawson, V. L., and Dawson, T. M. (2000) *Proc. Natl. Acad. Sci. U. S. A.* **97**, 13354–13359
14. Leroy, E., Boyer, R., Auburger, G., Leube, B., Ulm, G., Mezey, E., Harta, G., Brownstein, M. J., Jonnalagada, S., Chernova, T., Dehejia, A., Lavedan, C., Gasser, T., Steinbach, P. J., Wilkinson, K. D., and Polymeropoulos, M. H. (1998) *Nature* **395**, 451–452
15. Larsen, C. N., Krantz, B. A., Wilkinson, K. D. (1998) *Biochemistry* **37**, 3358–3368
16. Liu, Y., Fallon, L., Lashuel, H. A., Liu, Z., and Lansbury, P. T., Jr. (2002) *Cell* **111**, 209–218
17. Spillantini, M. G., Schmidt, M. L., Lee, V. M., Trojanowski, J. Q., Jakes, R., and Goedert, M. (1997) *Nature* **388**, 839–840
18. Mezey, E., Dehejia, A., Harta, G., Papp, M. I., Polymeropoulos, M. H., and Brownstein, M. J. (1998) *Nat. Med.* **4**, 755–757
19. Polymeropoulos, M. H., Lavedan, C., Leroy, E., Ide, S. E., Dehejia, A., Dutra, A., Pike, B., Root, H., Rubenstein, J., Boyer, R., Stenroos, E. S., Chandrasekharappa, S., Athanassiadou, A., Papapetropoulos, T., Johnson, W. G., Lazzarini, A. M., Duvoisin, R. C., Di Iorio, G., Golbe, L. I., and Nussbaum, R. L. (1997) *Science* **276**, 2045–2047
20. Kruger, R., Kuhn, W., Muller, T., Woitalla, D., Graeber, M., Kosel, S., Przuntek, H., Epplen, J. T., Schols, L., and Riess, O. (1998) *Nat. Genet.* **18**, 106–108
21. Baba, M., Nakajo, S., Tu, P. H., Tomita, T., Nakaya, K., Lee, V. M., Trojanowski, J. Q., and Iwatsubo, T. (1998) *Am. J. Pathol.* **152**, 879–884
22. Spillantini, M. G., Crowther, R. A., Jakes, R., Hasegawa, M., and Goedert, M. (1998) *Proc. Natl. Acad. Sci. U. S. A.* **95**, 6469–6473
23. Feany, M. B., and Bender, W. W. (2000) *Nature* **404**, 394–398
24. Auluck, P. K., Chan, H. Y., Trojanowski, J. Q., Lee, V. M., and Bonini, N. M. (2002) *Science* **295**, 865–868
25. Masliah, E., Rockenstein, E., Veinberga, I., Mallory, M., Hashimoto, M., Takeda, A., Sagara, Y., Sisk, A., and Mucke, L. (2000) *Science* **287**, 1265–1269
26. van der Putten, H., Wiederhold, K. H., Probst, A., Barbieri, S., Mistl, C., Danner, S., Kauffmann, S., Hofele, K., Spooren, W. P., Ruegg, M. A., Lin, S., Caroni, P., Sommer, B., Tolnay, M., and Bilbe, G. (2000) *J. Neurosci.* **20**, 6021–6029
27. Kahle, P. J., Neumann, M., Ozmen, L., Muller, V., Jacobsen, H., Schindzielorz, A., Okochi, M., Leimer, U., van der Putten, H., Probst, A., Kremmer, E., Kretzschmar, H. A., and Haass, C. (2000) *J. Neurosci.* **20**, 6365–6373
28. Kahle, P. J., Neumann, M., Ozmen, L., Muller, V., Odoy, S., Okamoto, N., Jacobsen, H., Iwatsubo, T., Trojanowski, J. Q., Takahashi, H., Wakabayashi, K., Bogdanovic, N., Riederer, P., Kretzschmar, H. A., and Haass, C. (2001) *Am. J. Pathol.* **159**, 2215–2225
29. Giasson, B. I., Duda, J. E., Quinn, S. M., Zhang, B., Trojanowski, J. Q., and Lee, V. M. (2002) *Neuron* **34**, 521–533
30. Lee, M. K., Stirling, W., Xu, Y., Xu, X., Qui, D., Mandir, A. S., Dawson, T. M., Copeland, N. G., Jenkins, N. A., and Price, D. L. (2002) *Proc. Natl. Acad. Sci. U. S. A.* **99**, 8968–8973
31. Engelender, S., Kaminsky, Z., Guo, X., Sharp, A. H., Amaravi, R. K., Kleiderlein, J. J., Margolis, R. L., Troncoso, J. C., Lanahan, A. A., Worley, P. F., Dawson, V. L., Dawson, T. M., and Ross, C. A. (1999) *Nat. Genet.* **22**, 110–114
32. Neystat, M., Rzhetskaya, M., Kholodilov, N., and Burke, R. E. (2002) *Neurosci. Lett.* **325**, 119–123
33. Kawamata, H., McLean, P. J., Sharma, N., and Hyman, B. T. (2001) *J. Neurochem.* **77**, 929–934
34. Ribeiro, C. S., Carneiro, K., Ross, C. A., Menezes, J. R., and Engelender, S. (2002) *J. Biol. Chem.* **277**, 23927–23933
35. Chung, K. K., Zhang, Y., Lim, K. L., Tanaka, Y., Huang, H., Gao, J., Ross, C. A., Dawson, V. L., and Dawson, T. M. (2001) *Nat. Med.* **7**, 1144–1150
36. O'Farrell, C., Murphy, D. D., Petrucelli, L., Singleton, A. B., Hussey, J., Farrer,

M., Hardy, J., Dickson, D. W., and Cookson, M. R. (2001) *Brain Res. Mol. Brain Res.* **97,** 94–102

37. Lee, G., Junn, E., Tanaka, M., Kim, Y. M., and Mouradian, M. M. (2002) *J. Neurochem.* **83,** 346–352

38. Wakabayashi, K., Engelender, S., Tanaka, Y., Yoshimoto, M., Mori, F., Tsuji, S., Ross, C. A., and Takahashi, H. (2002) *Acta Neuropathol.* **103,** 209–214

39. Wakabayashi, K., Engelender, S., Yoshimoto, M., Tsuji, S., Ross, C. A., and Takahashi, H. (2000) *Ann. Neurol.* **47,** 521–523

40. Niwa, J.-i., Ishigaki, S., Doyu, M., Suzuki, T., Tanaka, K., and Sobue, G. (2001) *Biochem. Biophys. Res. Commun.* **281,** 706–713

41. Morett, E., and Bork, P. (1999) *Trends Biochem. Sci.* **24,** 229–231

42. Moynihan, T. P., Ardley, H. C., Nuber, U., Rose, S. A., Jones, P. F., Markham, A. F., Scheffner, M., and Robinson, P. A. (1999) *J. Biol. Chem.* **274,** 30963–30968

43. Ardley, H. C., Tan, N. G., Rose, S. A., Markham, A. F., and Robinson, P. A. (2001) *J. Biol. Chem.* **276,** 19640–19647

44. Niwa, J.-i., Ishigaki, S., Hishikawa, N., Yamamoto, M., Doyu, M., Murata, S., Tanaka, K., Taniguchi, N., and Sobue, G. (2002) *J. Biol. Chem.* **277,** 36793–36798

45. Hishikawa, N., Hashizume, Y., Yoshida, M., and Sobue, G. (2001) *Neuropathol. Appl. Neurobiol.* **27,** 362–372

46. Lee, M., Hyun, D., Halliwell, B., and Jenner, P. (2001) *J. Neurochem.* **76,** 998–1009

47. Braak, H., Sandmann-Keil, D., Gai, W., and Braak, E. (1999) *Neurosci. Lett.* **265,** 67–69

48. Takahashi, H., and Wakabayashi, K. (2001) *Neuropathology* **21,** 315–322

49. Schlossmacher, M. G., Frosch, M. P., Gai, W. P., Medina, M., Sharma, N., Forno, L., Ochiishi, T., Shimura, H., Sharon, R., Hattori, N., Langston, J. W., Mizuno, Y., Hyman, B. T., Selkoe, D. J., and Kosik, K. S. (2002) *Am. J.*

Pathol. **160,** 1655–1667

50. Lee, H. J., and Lee, S. J. (2002) *J. Biol. Chem.* **277,** 48976–48983

51. Klein, W. L., Krafft, G. A., and Finch, C. E. (2001) *Trends Neurosci.* **24,** 219–224

52. Bucciantini, M., Giannoni, E., Chiti, F., Baroni, F., Formigli, L., Zurdo, J., Taddei, N., Ramponi, G., Dobson, C. M., and Stefani, M. (2002) *Nature* **416,** 507–511

53. Conway, K. A., Lee, S. J., Rochet, J. C., Ding, T. T., Williamson, R. E., and Lansbury, P. T., Jr. (2000) *Proc. Natl. Acad. Sci. U. S. A.* **97,** 571–576

54. Goldberg, M. S., and Lansbury, P. T., Jr. (2000) *Nat. Cell Biol.* **2,** 115–119

55. Shimura, H., Schlossmacher, M. G., Hattori, N., Frosch, M. P., Trockenbacher, A., Schneider, R., Mizuno, Y., Kosik, K. S., and Selkoe, D. J. (2001) *Science* **293,** 263–269

56. Okochi, M., Walter, J., Koyama, A., Nakajo, S., Baba, M., Iwatsubo, T., Meijer, L., Kahle, P. J., and Haass, C. (2000) *J. Biol. Chem.* **275,** 390–397

57. Fujiwara, H., Hasegawa, M., Dohmae, N., Kawashima, A., Masliah, E., Goldberg, M. S., Shen, J., Takio, K., and Iwatsubo, T. (2002) *Nat. Cell Biol.* **4,** 160–164

58. Valente, E. M., Bentivoglio, A. R., Dixon, P. H., Ferraris, A., Ialongo, T., Frontali, M., Albanese, A., and Wood, N. W. (2001) *Am. J. Hum. Genet.* **68,** 895–900

59. Valente, E. M., Brancati, F., Ferraris, A., Graham, E. A., Davis, M. B., Breteler, M. M., Gasser, T., Bonifati, V., Bentivoglio, A. R., De Michele, G., Durr, A., Cortelli, P., Wassilowsky, D., Harhangi, B. S., Rawal, N., Caputo, V., Filla, A., Meco, G., Oostra, B. A., Brice, A., Albanese, A., Dallapiccola, B., and Wood, N. W. (2002) *Ann. Neurol.* **51,** 14–18

60. Marin, I., and Ferrus, A. (2002) *Mol. Biol. Evol.* **19,** 2039–2050

61. Gearhart, D. A., Toole, P. F., and Beach, J. W. (2002) *Neurosci. Res.* **44,** 255–265

Hsp105α Suppresses the Aggregation of Truncated Androgen Receptor with Expanded CAG Repeats and Cell Toxicity*

Keiichi Ishihara‡, Nobuyuki Yamagishi‡, Youhei Saito‡, Hiroaki Adachi§, Yasushi Kobayashi§, Gen Sobue§, Kenzo Ohtsuka¶, and Takumi Hatayama‡||

From the ‡Department of Biochemistry, Kyoto Pharmaceutical University, 5 Nakauchi-cho, Misasagi, Yamashina-ku, Kyoto 607-8414, the §Department of Neurology, Nagoya University Graduate School of Medicine, 65 Tsurumai-cho Showa-ku, Nagoya 466-8550, and the ¶Department of Environmental Biology, College of Bioscience and Biotechnology, Chubu University, Matsumoto-cho 1200, Kasugai 487-8501, Japan

Spinal and bulbar muscular atrophy (SBMA) is a neurodegenerative disorder caused by the expansion of a polyglutamine tract in the androgen receptor (AR). The N-terminal fragment of AR containing the expanded polyglutamine tract aggregates in cytoplasm and/or in nucleus and induces cell death. Some chaperones such as Hsp40 and Hsp70 have been identified as important regulators of polyglutamine aggregation and/or cell death in neuronal cells. Recently, Hsp105α, expressed at especially high levels in mammalian brain, has been shown to suppress apoptosis in neuronal cells and prevent the aggregation of protein caused by heat shock in vitro. However, its role in polyglutamine-mediated cell death and toxicity has not been studied. In the present study, we examined the effects of Hsp105α on the aggregation and cell toxicity caused by expansion of the polyglutamine tract using a cellular model of SBMA. The transient expression of truncated ARs (tARs) containing an expanded polyglutamine tract caused aggregates to form in COS-7 and SK-N-SH cells and concomitantly apoptosis in the cells with the nuclear aggregates. When Hsp105α was overexpressed with tAR97 in the cells, Hsp105α was colocalized to aggregates of tAR97, and the aggregation and cell toxicity caused by expansion of the polyglutamine tract were markedly reduced. Both β-sheet and α-helix domains, but not the ATPase domain, of Hsp105α were necessary to suppress the formation of aggregates in vivo and in vitro. Furthermore, Hsp105α was found to localize in nuclear inclusions formed by ARs containing an expanded polyglutamine tract in tissues of patients and transgenic mice with SBMA. These findings suggest that overexpression of Hsp105α suppresses cell death caused by expansion of the polyglutamine tract without chaperone activity, and the enhanced expression of the essential domains of Hsp105α in brain may provide an effective therapeutic approach for CAG repeat diseases.

Spinal and bulbar muscular atrophy (SBMA)[1] is an X-linked motor neuropathy characterized by proximal muscle atrophy,

weakness, contraction fasciculation, and bulbar involvement (1, 2). In SBMA patients, a normally polymorphic CAG repeat (10–36 CAGs) in exon 1 of the androgen receptor (AR) gene expands to 40–62 CAGs (3), and nuclear inclusions containing mutant and truncated ARs with an expanded polyglutamine tract are characteristically found in the residual motor neurons in the brain stem and spinal cord (4) as well as in the skin, testis, and other visceral organs (5). In addition to SBMA, expansions of CAG repeats encoding polyglutamine tracts in unrelated proteins are responsible for at least another eight different neurodegenerative diseases including Huntington's disease (6), dentatorubral pallidoluysian atrophy (7, 8), Machado-Joseph disease (9), and several types of spinocerebellar ataxia (10–15). All of these disorders show a late onset of neurological symptoms with progressive neuronal dysfunction and eventual neuronal loss, although the susceptible regions in the nervous system differ among the various disorders. The appearance of intranuclear aggregates/inclusions in neurons is associated with these neurodegenerative diseases. The intranuclear inclusions contain the insoluble protein aggregates of abnormal proteins or their fragments, heat shock proteins, and components of the ubiquitin-dependent proteasome degradation pathway (16, 17). Although the nature of the toxic insult of a polyglutamine mutation and its cell-biological consequences in each disease are unclear, it is possible that the polyglutamine expansion interferes with basic cellular processes such as transcription, protein degradation, and survival/death signaling (17). However, the exact role of these protein aggregates in polyglutamine pathology is still controversial because large polyglutamine aggregates may provide an advantage over small oligomers by exposing less potentially dangerous protein surfaces (18). The cellular components involved in protein folding and degradation are also associated with intracellular inclusions in other neurodegenerative diseases not caused by polyglutamine expansion, including Alzheimer's, Parkinson's, and the prion diseases (19), which suggests that common mechanistic principles may underlie these misfolding diseases in general.

A considerable effort has been made to find molecules that suppress polyglutamine aggregation and cell death/toxicity for therapeutic purposes (20–22). In general, the misfolding and aggregation of proteins are prevented by molecular chaperones (23, 24). Some molecular chaperones such as heat shock protein (Hsp) 70 and Hsp40 have recently been identified as important regulators of polyglutamine aggregation and/or cell death in in

|| To whom correspondence should be addressed. Fax: 81-75-595-4758; E-mail: hatayama@mb.kyoto-phu.ac.jp.

[1] The abbreviations used are: SBMA, spinal and bulbar muscular atrophy; AR, androgen receptor; BSA, bovine serum albumin; GFP, green fluorescent protein; HA, hemagglutinin; PBS, phosphate-buffered saline; tAR, truncated androgen receptor; TUNEL, terminal nucleotidyl transferase-mediated UTP nick end labeling.

TABLE I
*Primers used for construction of expression plasmids for Hsp105α
deletion mutants*

Expression in mammalian cell
Hsp105N1 (a.a. 1–392)
  Sense: 5'-CGGAGAAAGAATTGCACACTG-3'
  Antisense: 5'-TCTAGAGGGCCCTTCGAACAA-3'
Hsp105N2 (a.a. 1–511)
  Sense: 5'-GGGGTACCCAGCCATGTCGGTGGTT-3'
  Antisense: 5'-TCTAGAGGGCCCTTCGAACAA-3'
Hsp105N3 (a.a. 1–606)
  Sense: 5'-TAACTGCCATACCAAGTTGGC-3'
  Antisense: 5'-TCTAGAGGGCCCTTCGAACAA-3'
Hsp105C1 (a.a. 605–858)
  Sense: 5'-GGGGATCCACCATGCTCGAGGCAGACATGGAATGT-3'
  Antisense: 5'-GCTCTAGACCTAGTCCAGGTCCATGTTGAC-3'
Hsp105C2 (a.a. 511–858)
  Sense: 5'-GGGGATCCACCATGCTCGAGGCAGACATGGAATGT-3'
  Antisense: 5'-GCTCTAGACCTAGTCCAGGTCCATGTTGAC-3'
Hsp105C3 (a.a. 386–858)
  Sense: 5'-GGGGATCCACCATGCCGGCATTTAAAGTTAGAGAG-3'
  Antisense: 5'-GCTCTAGACCTAGTCCAGGTCCATGTTGAC-3'
Hsp105Δβ (a.a. 1–392 + a.a. 551–858)
  Sense: 5'-CTCGAGGCAGACATGGAATGTCCA-3'
  Antisense: 5'-AGAAAGAATTGCACACTGCAGTGCAC-3'
Hsp105ΔβL (a.a. 1–392 + a.a. 605–858)
  Sense: 5'-GGGAGAGACCTTCTTAACATGTATATTG-3'
  Antisense: 5'-AGAAAGAATTGCACACTGCAGTGCAC-3'
Hsp105ΔL (a.a. 1–511 + a.a. 605–858)
  Sense: 5'-GGGAGAGACCTTCTTAACATGTATATTG-3'
  Antisense: 5'-AGAGGAGCCATCCTCTTCCTCGGT-3'
Expression in bacterial cell
Hsp105Δβ
  Sense: 5'-CTCGAGGCAGACATGGAATGTCCA-3'
  Antisense: 5'-AGAAAGAATTGCACACTGCAGTGCAC-3'
Hsp105ΔβL
  Sense: 5'-GGGAGAGACCTTCTTAACATGTATATTG-3'
  Antisense: 5'-AGAAAGAATTGCACACTGCAGTGCAC-3'
Hsp105ΔL
  Sense: 5'-GGGAGAGACCTTCTTAACATGTATATTG-3'
  Antisense: 5'-AGAGGAGCCATCCTCTTCCTCGGT-3'

(A) COS-7 cells

(B) SK-N-SH cells

FIG. 1. **Truncated AR containing an expanded polyglutamine tract is accumulated as aggregates in COS-7 and SK-N-SH cells.** Expression plasmids for N-terminal fragments of AR containing various lengths of polyglutamine tract (tAR24, tAR65, and tAR97, 0.5 μg each) were transiently introduced into COS-7 (A) or SK-N-SH cells (B), and the cells were incubated further for 72 h. Each *upper panel* shows typical images of fluorescence of GFP which is fused to the C terminus of truncated AR, and each *lower graph* represents the rates of cells with aggregates *versus* GFP-positive cells at various times after transfection. Values represent the mean of duplicate experiments.

vitro assays (25), in cultured mammalian cells (26–31), in a *Drosophila* model (32) and in transgenic mice (33, 34). Hsp27 was also identified as a suppressor of polyglutamine-mediated cell death using a cellular model of Huntington's disease (35). However, because Hsp70/40 and Hsp27 suppressed polyglutamine-mediated death without suppressing polyglutamine aggregation in some experimental systems (35, 36), elucidation of the ways in which Hsps protect cells against polyglutamine mutations might be of relevance for other neurodegenerative conditions in which pathology is associated with protein deposition in neuronal cells.

Hsp105α is highly conserved in organisms from yeast to human (37–42) and is expressed in various tissues of mammals, but especially at high levels in brain (43). Recently, Hsp105α was demonstrated to have antiapoptotic properties for neuronal survival (44). Furthermore, Hsp105α prevents the aggregation of thermal denatured protein *in vitro* (45). However, its role in polyglutamine-mediated cell death/toxicity has not been studied. In the present study, we examined the role of Hsp105α in the context of polyglutamine aggregation and cell death using a cellular model of SBMA and demonstrate that Hsp105α without chaperone activity protects cells against polyglutamine-mediated cell death by reducing polyglutamine-protein aggregation. These findings suggest an important role for Hsp105α in preventing neurodegenerative diseases associated with polyglutamine expansions.

EXPERIMENTAL PROCEDURES

Plasmids—We used constructs expressing the N-terminal fragment of the AR fused to green fluorescence protein (GFP) containing 24, 65, or 97 CAG repeats (tAR24, tAR65, and tAR97, respectively) as a cellular model of SBMA (29), human Hsp70 (pCMV-Hsp70) (46), and Hsp40
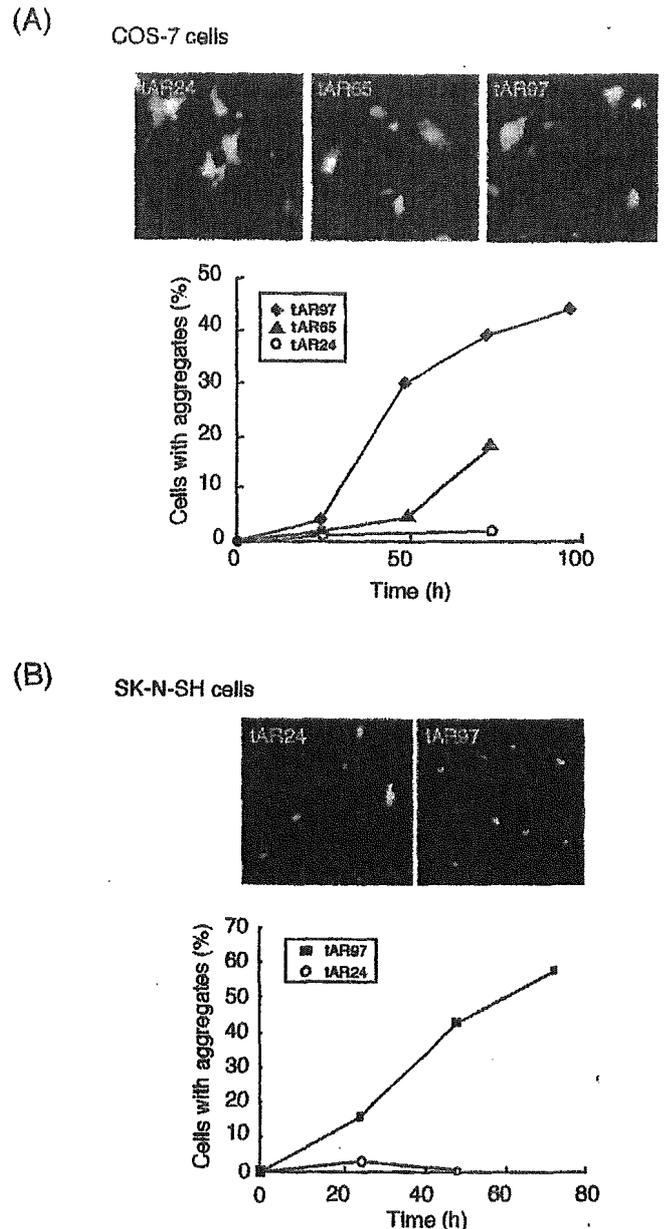
(pRC-Hsp40) (29) in mammalian cells. The constructs expressing Hsp105α (pcDNA105α) and Myc-epitope/His-tagged Hsp105α (pcDNA105α-mycHis) in mammalian cells were generated by ligating a full-length mouse Hsp105α cDNA (38) into pcDNA3.1 (Invitrogen) at BamHI and EcoRI sites and pcDNA3.1(+)-mycHis vector (Invitrogen) at XbaI and KpnI sites, respectively. The constructs expressing Hsp105N1–N3, Δβ, ΔL, and ΔβL in mammalian cells were generated by self-ligation of DNA made by PCR using pcDNA105α-mycHis (Hsp105N1–N3) or pcDNA105α (Hsp105Δβ, ΔL, ΔβL, and C1–C3) as template DNA and a specific set of primers (Table I).

We used a construct expressing GST- and HA-tagged tAR65 (GST-tAR65-HA) in bacterial cells (47). The constructs expressing HSP105α deletion mutants in bacterial cells were generated by ligating insert DNA made by PCR using pTrcHis105-1 (45) as a template DNA and a specific set of primers (Table I) into pTrcHisA vector (Invitrogen) at the KpnI site.

(A)

(B)

FIG. 2. **Apoptosis occurs in cells with intranuclear aggregates.** *A,* COS-7 cells were transfected with the expression plasmid for tAR24 (+ *tAR24*) or tAR97 (+ *tAR97*) and incubated further for 48 or 72 h. Then cells were fixed and stained with Hoechst 33342. Rates of cells with condensed chromatin *versus* GFP-positive cells are presented. *B,* COS-7 cells were transfected with the expression plasmid for tAR97 and incubated further for 72 h. Rates of apoptotic cells *versus* cells with aggregates in nuclei and/or cytoplasms are presented. Values in *A* and *B* represent the mean ± S.D. of three independent experiments. *C,* fragmentation of DNA in nuclei was evaluated by TUNEL methods 72 h after the transfection of tAR97. *DIC* represents a difference interference contrast image of cells.

(C)
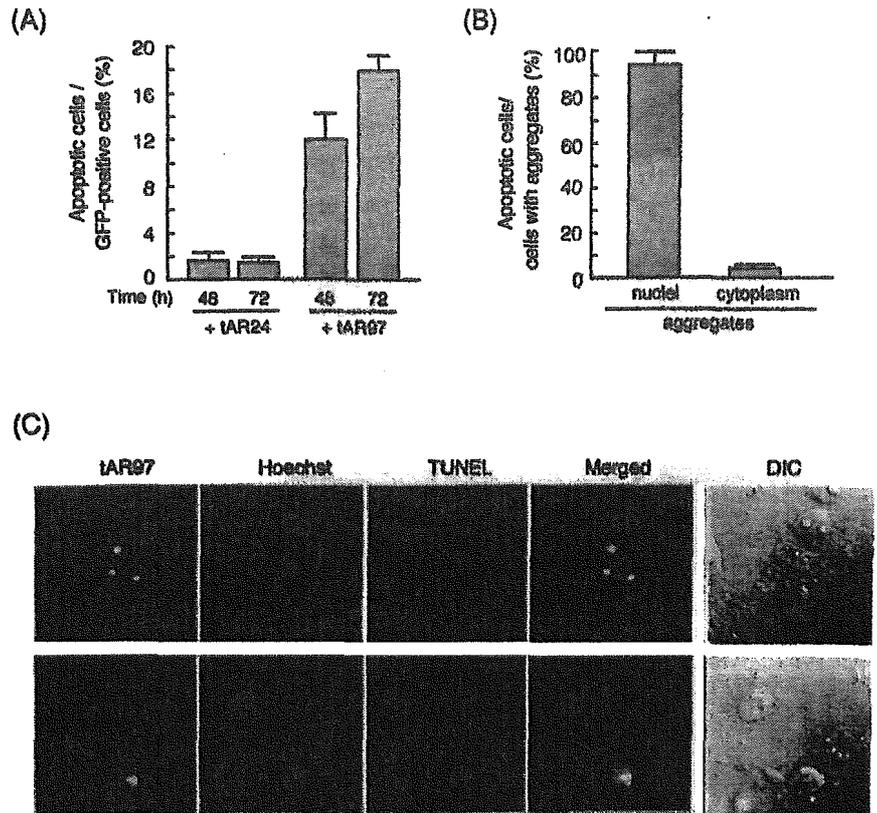
Cell Culture and Transfection—African green monkey kidney cells (COS-7) and human neuroblastoma cells (SK-N-SH) were supplied from Riken cell bank. COS-7 cells were maintained in Dulbecco's modified Eagle's medium (Nissui Pharmaceutical) supplemented with 10% fetal bovine serum. SK-N-SH cells were maintained in α-minimal essential medium (Invitrogen) with 10% fetal bovine serum. For transfection of plasmid DNA, cells were grown on coverslips to 70–80% confluence and washed twice with Opti-MEM (Invitrogen). Then plasmid DNA was transfected into cells with DMRIE-C reagent (Invitrogen) for 14–18 h, according to the manufacturer's instructions.

Indirect Immunofluorescence—COS-7 cells grown on coverslips were washed with phosphate-buffered saline without Ca^{2+} and Mg^{2+} (PBS(−)) and fixed with 4% paraformaldehyde for 30 min at room temperature. These cells were washed with PBS(−) and incubated with blocking solution containing 3% bovine serum albumin (BSA) in PBS(−) at room temperature for 1 h. Then rabbit anti-human Hsp105 (48) or mouse anti-Hsp70 monoclonal antibody (Sigma) at a 1:300 dilution was added to the coverslips and incubated in a moist chamber at 37 °C for 1 h. After a wash with PBS(−), rhodamine-conjugated goat anti-rabbit or mouse IgG antibody (Molecular Probes) at a 1:50 dilution was added to the coverslips, and they were incubated further at 37 °C for 1 h. After another wash with PBS(−), cells were observed using a confocal laser scanning microscope (Zeiss).

Analysis of Aggregation in Vivo—COS-7 cells transfected with expression plasmid for tAR24, tAR65, or tAR97 were washed with PBS(−) and fixed with 4% paraformaldehyde at room temperature. Cells on coverslips were washed with PBS(−) and stained with 10 μM Hoechst 33342 for 15 min at room temperature. The cells were washed with PBS(−) and then examined using a confocal laser scanning microscope. The number of transfected cells with visible aggregates and the number of transfected cells without aggregates were counted independently in randomly chosen microscopic fields in different areas of a coverslip. Approximately 300–600 transfected cells were analyzed for data in each experiment.

Detection of the Apoptotic Cells—The apoptotic cells were identified by their nuclear morphology and the terminal nucleotidyl transferase-mediated UTP nick end labeling (TUNEL) method (29). Nuclear morphology was examined by staining with Hoechst 33342. The TUNEL method was performed using a DeadEnd™ apoptosis detection kit (Promega) according to the manufacturer's instructions. Briefly, cells were fixed with 4% paraformaldehyde at 72 h after transfection. Fixed cells were incubated with biotinylated deoxynucleotides, then stained with

streptavidin-rhodamine conjugate (Molecular Probes) and Hoechst 33342. Cells were then observed by confocal laser scan microscopy.

Western Blotting Analysis—Cells were lysed with a solution containing 0.1% SDS at 72 h after transfection. The cellular proteins (15 μg) were separated by 7.5% SDS-PAGE and blotted onto a nitrocellulose membrane. The membrane was incubated with rabbit anti-human Hsp105 (37) or mouse anti-Hsp70 (Sigma) antibody, then incubated with horseradish peroxidase-conjugated anti-rabbit IgG (Santa Cruz) for Hsp105 or anti-mouse IgG (Santa Cruz) for Hsp70 at a 1:2,000 dilution. These proteins were detected using the enhanced chemiluminescence (ECL) detection system (Amersham Biosciences).

Protein Purification—GST-tAR65-HA was expressed in BL21 bacterial cells on addition of 1 mM isopropyl-β-D-thiogalactopyranoside. Cells were collected and resuspended in ice-cold TEGM buffer (10 mM Tris-HCl, pH 7.4, 1 mM EDTA, 10% glycerol, and 10 mM sodium molybdate). Cells were then sonicated for 1 min and centrifuged for 30 min at 10,000 × g. To purify GST-tagged proteins, the supernatants were mixed with glutathione-Sepharose 4B (Amersham Biosciences) and incubated at 4 °C for 1 h. The Sepharose beads were then washed with PBS(−) and eluted with 10 mM reduced glutathione. Wild-type Hsp105α and its mutants were purified as His-tagged proteins by successive Ni^{2+}-agarose (Invitrogen) and Mono Q anion exchange column (Amersham Biosciences) chromatographies, as described previously (45).

Detection of Aggregates of Truncated AR in Vitro—GST-tAR65-HA (1 μM) was incubated with Hsp105α, its mutants, or BSA in 20 μl of buffer A (25 mM Tris-HCl, pH 7.5, 150 mM NaCl, 1 mM dithiothreitol, and 1 mM phenylmethylsulfonyl fluoride) at 30 °C for 12 h in the presence of 2 mM ADP. The reaction was stopped by the addition of 20 μl of a solution containing 2% SDS and 100 mM dithiothreitol, and the mixtures were heated at 98 °C for 5 min. After the addition of 200 μl of a 1% SDS solution, the mixture was filtered through a 0.2-μm cellulose acetate membrane (Advantec). Aggregates on the membrane were incubated with anti-HA tag antibody (1:500, Santa Cruz) then with peroxidase-conjugated anti-mouse IgG antibody (1:2000) and detected with an ECL detection system (Santa Cruz).

Immunohistochemistry—We perfused 20 ml of a 4% paraformaldehyde fixative in 0.1 M phosphate buffer, pH 7.4, through the left cardiac ventricle of SBMA transgenic mice (49) deeply anesthetized with ketamine-xylazine, postfixed tissues overnight in 10% phosphate-buffered formalin, and processed tissues for paraffin embedding. Then, 4-μm thick tissue sections were deparaffinized, dehydrated with alcohol, and